

Renate Høvik Berge

Accessing Flexibility in Batteries Through a Local Flexibility Market

Master's thesis in Energy and Environmental Engineering

Supervisor: Jayaprakash Rajasekharan

Co-supervisor: Sigurd Bjarghov

July 2022

Renate Høvik Berge

Accessing Flexibility in Batteries Through a Local Flexibility Market

Master's thesis in Energy and Environmental Engineering
Supervisor: Jayaprakash Rajasekharan
Co-supervisor: Sigurd Bjarghov
July 2022

Norwegian University of Science and Technology
Faculty of Information Technology and Electrical Engineering
Department of Electric Power Engineering

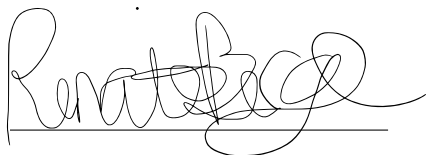
Preface

This master thesis was completed in July 2022 and is the final part of the Master of Technology in Energy and Environmental Engineering. The master thesis accounts for 30 credits in the 10th semester of the degree. The master thesis was given by the Department of Electric Power Engineering at the Norwegian University of Science and Technology (NTNU).

First and foremost I would like to thank my supervisor associate professor Jayaprakash Rajasekharan for guidance, support and helpful discussion. I would also like to thank my co-supervisor PhD-candidate Sigurd Bjarhov for countless of discussion (relevant and not), programming guidance and countless of helpful inputs throughout the writing process.

I would also like to thank my parents for their constant support, love and motivation throughout my six years as a student. Lastly, a thanks to all of my fellow students and friends for six memorable years as a student at NTNU.

Trondheim, 11th of July 2022

A handwritten signature in black ink, appearing to read 'Renate Høvik Berge', written over a horizontal line.

Renate Høvik Berge

Abstract

The *power quality regulation* states that the distribution system operator is responsible for maintaining the power quality in the grid and ensuring that the voltage quality is within statutory limits. Due to environmental issues and a demand for more efficient energy generation the power system is transforming into a more decentralized system resulting in more intermittent power generation and distributed generation. This results in challenges in the distribution grid, such as under-voltage issues. The use of battery energy storage in the distribution grid provides a reliable energy source to be used for e.g. voltage control. The flexibility in battery energy storage systems can be made accessible for the distribution system operator through local flexibility markets.

This master thesis therefore presents the network model of a case study network with under-voltage issues. The under-voltage issues are evaluated for three load profile scenarios and the results are used to procure the flexibility demand for the load profile scenarios, consider two set voltage limits at 0.95 pu and 0.9 pu. These voltage limits reflect the DSO responsibility for ensuring the power quality in the distribution grid and the responsibility for ensuring that the voltage quality is within statutory limits. A two-stage stochastic optimization model was created with goal of obtaining enough flexibility, through a battery, to cover the flexibility demands procured, and thereby avoid violating the set voltage limits. The objective of the model is to minimize the total cost for the distribution system operator considering the cost of booking and activating flexibility through two flexibility options, LongFlex and ShortFlex, and also considering the cost of battery degradation.

The use of various load profile scenarios in the network model resulted in varying degree of under-voltage issues, considering voltage magnitude and the duration of the issues. The use of the flexibility demands procured, by the use of the under-voltage limit, in the optimization model verified that the model booked and activated enough flexibility to cover the demands. The use of ShortFlex and LongFlex varied with the cost of booking and activation, for both of the cost profiles. The battery discharged enough power to cover the demand and various segments in battery are activated. However, the model resulted in low cost for the distribution system operator as a result of operating with small amount of power and a overdimensioned battery. The use of the power quality limit resulted in a very high flexibility demand for each scenario, and the use of these demands in the optimization model resulted in an infeasible model. This was a result of the constant flexibility demands, which did not allow for any battery charging. In situations with a great demand more batteries must be considered or other options for reinforcing the grid.

Sammendrag

Netteieren, eller distribusjonssystemoperatøren, er ansvarlig for å operere og vedlikeholde distribusjonsnettene. I *forskrift om leveringskvalitet* er det fastsatt at det er netteieren som er ansvarlig for å opprettholde kraft- og spenningskvaliteten i nettet, dette innebærer at spenningen skal være innenfor lovbestemte grenser. På grunn av den pågående klimakrisen og behovet for mer effektiv kraftproduksjon blir strømmettet mer og mer desentralisert. Dette medfører en økt andel varierende fornybar kraftproduksjon og mer kraftproduksjon koblet til distribusjonsnettene. Den pågående endringen av strømmettet medfører ulike spenningproblemer som f.eks. under-spenningsproblemer. Bruken av batteri i distribusjonsnettene gir tilgang på en pålitelig energikilde som kan benyttes til f.eks. spenningsregulering. Fleksibiliteten i batteriene kan tilgjengelig gjøres gjennom lokale fleksibilitet marked.

Denne masteren presenterer derfor en modell av et casestudie nettverket med under-spenningsproblemer. Spenningsproblemene vurderes ut i fra tre ulike last profil scenario og resultatene benyttes for å skaffe fleksibilitetsbehovet for de ulike scenarioene, med hensyn til to ulike spenningsgrenser, på 0.95 pu og 0.90 pu. Spenningsgrensene ble satt for å reflektere netteierens ansvar for å opprettholde kraft- og spenningskvaliteten i nettet.

En to-steg stokastisk optimeringsmodell ble laget med et mål om å skaffe nok fleksibilitet, fra et batteri, til å dekke fleksibilitetsbehovene ved de tre last profil scenarioene. Objektivet til modellen er å minimere netteieren utgifter med hensyn på kostnaden av å booke og aktivere fleksibilitet gjennom to fleksibilitetsmuligheter, LongFlex og ShortFlex, og samtidig ta hensyn til kostandene ved nedbrytingen av de ulike segmentene i batteriet.

Ved å benytte fleksibilitetsbehovet skaffet ved bruk av under-spenningsgrensen og to ulike profiler for fleksibilitetskostnader i optimeringsmodellen gir en bekreftelse på at modellen fungerer slik den skal, ettersom det aktiveres nok fleksibilitet til å dekke behovet. Det benyttes både ShortFlex og LongFlex avhenging av prisen på aktivering og booking. Modellen trekker nok kraft fra batteriet til å dekke behovet og ulike segmenter i batteriet blir aktivert. Den totale kostnaden for netteieren er veldig lav, men dette kommer av at batteriet er overdimensjonert og av det lave fleksibilitetsbehovet. Ved å benytte fleksibilitetsbehovene fra kraft-kvalitetsgrense er ikke modellen løselig, og dette er på grunn av det konstante fleksibilitetsbehovet, ettersom dette betyr at batteriet ikke får muligheten til å lade. I slike situasjoner kan det være mulig å benytte flere batterier eller vurdere andre metoder for å styrke nettet.

Table of Contents

- Preface i
- Abstract ii
- Sammendrag iii
- Table of Contents iv
- List of Abbreviations vi
- List of Symbols viii
- List of Figures xi
- List of Tables xii

- 1 Introduction 1**
- 1.1 Background and Motivation 1
- 1.2 Scope of Work 2
- 1.3 Contribution 2
- 1.4 Thesis Outline 3

- 2 Theoretical Background 4**
- 2.1 Distribution Grid 4
 - 2.1.1 Power Quality Regulation 5
 - 2.1.2 From a Centralized to a Decentralized Power System 5
 - 2.1.3 Power Quality Challenges 7
 - 2.1.4 Voltage Control in the Distribution System 7
- 2.2 Flexibility 8
 - 2.2.1 Flexibility Resources 8
 - 2.2.2 Distribution System Flexibility 10
 - 2.2.3 Local Flexibility Market 10
 - 2.2.4 NODES 11
- 2.3 Battery Energy Storage Systems 12
 - 2.3.1 BESS in Distribution Systems 12
 - 2.3.2 Characteristics 13
 - 2.3.3 Stress Factors in Battery Degradation 13
 - 2.3.4 Modeling of Battery Degradation in Optimization 13
- 2.4 Power Flow and Stochastic Programming 16
 - 2.4.1 AC Power Flow Analysis 16
 - 2.4.2 Stochastic Programming for Optimization 20

- 3 Case Study 22**

3.1	Network Overview	22
3.2	Load Profile Scenarios	23
3.3	Battery Case	24
4	Methodology	25
4.1	Network Modeling and Simulation	25
4.1.1	Software: PandaPower	25
4.1.2	Test Feeder Overview	26
4.1.3	Network Modifications and Modeling	27
4.1.4	Network Simulation	30
4.2	Optimization Model	30
4.2.1	Software: Pyomo and Gurobi Optimizer	30
4.2.2	Two-Stage Stochastic Optimization Model	31
4.2.3	Model Limitations	35
4.2.4	Data	35
5	Results and Discussion	39
5.1	Network Model	39
5.1.1	Voltage Magnitude	39
5.1.2	Under-Voltage Issues	40
5.1.3	Power Quality Issues	42
5.1.4	Flexibility Demand	43
5.2	Optimization Model	44
5.2.1	Under-Voltage Issues	44
5.2.2	Power Quality	52
5.2.3	Optimization Model	52
6	Conclusion	53
	Further Work	55
	References	56
A	Network Model Data	i
A.1	Line Connections	i
A.2	Line Types Specifications	iii
A.3	Transformer Specifications	iii

List of Abbreviations

AC	Alternating Current
AVR	Automatic Voltage Regulating
BES	Battery Energy Storage
BESS	Battery Energy Storage System
BRP	Balance Responsible Party
CAES	Compressed Air Energy Storage
CAPEX	Capital Expenditure
CHP	Combined Heat and Power
DER	Distributed Energy Resource
DG	Distributed Generation
DOD	Depth of Discharge
DR	Demand Response
DSM	Demand-Side Management
DSO	Distribution System Operator
EBM	Element-Based Model
ESS	Energy Storage System
EU	European Union
EV	Electrical Vehicle
FEC	Full Equivalent Cycle
HES	Hydrogen Energy Storage

HV	High Voltage
HVAC	Heating, Ventilation and Air Conditioning
IEEE	(University of Kassel and Fraunhofer) Insitute for Energy Economics and Energy System Technology
LFM	Local Flexibility Market
LV	Low Voltage
MV	Medium Voltage
NVE	Norwegian Water Resources and Energy Directorate
OLTC	On-Load Tap Changer
OPEX	Operational Expenditure
PV	PhotoVoltaic
RCS	Remotely Controllable Switch
RES	Renewable Energy Source
SC	Shunt Capacitor
SOC	State of Charge
SOC	State of Health
SOP	Soft Open Point
SVC	Static Var Compensator
SVR	Step Voltage Regulator
TSO	Transmission System Operator
VPP	Virtual Power Plant
VVC	Volt/VAr Control

List of Symbols

δ	Voltage angle [°]
δ_t	Battery cycle depth [-]
ϵ	Error [-]
η_{dis}	Battery discharge efficiency [%]
κ_C	Battery cyclic aging factor [\$/cycle]
κ_K	Battery calendar aging factor [$1/\sqrt{\text{min}}$]
ϕ	Phase angle [°]
ϕ	Battery cycle life coefficient dependent ambient temperature [-]
Φ	Battery loss of cycle life [%]
$\cos(\phi)$	Powerfactor [-]
a, b	Battery cycle life coefficient dependent on DOD [-]
B	Battery degradation cost [\$/kWh]
B_c^n	Battery degradation cost per cycle c [\$/cycle]
C_{BC}	Battery capital cost involving replacement labor [-]
C_{BD}	Battery degradation cost [-]
c_j	Battery degradation cost per segment [\$/kWh]
C_t^r	C-rate per time step t [-]
DOD^t	Depth of discharge per time step t [-]
E	Battery roundtrip efficiency [%]
E^{B0}	Initial battery capacity [kWh]

E_t^B	Battery capacity in time step t [kWh]
$E^{B,cap}$	Actual energy capacity [kWh]
E_{BESS}^{max}	Maximum energy stored in the battery [MWh]
E^{total}	Total energy storage in battery [-]
FEC_t	Full equivalent cycle per time step t [cycles]
f_n	Remaining battery cycles to failure [cycles]
f_t^c	Cycle aging function [%/cycle]
J	Jacobian matrix [-]
J/j	Total amount of segments/current segment [-]
N/n	Number of buses [-]
L	Battery lifetime throughput [kWh]
L_{DOD}	Battery cycle life [cycles]
L_R	Rated battery cycle life [-]
L_{temp}	Number of cycle [-]
L_{VVP}	Battery cycle life VPP participation [-]
m	Battery cycle life coefficient dependent ambient temperature [-]
P	Active power [W]
P_t^B	Power discharge per time step t [kW]
P_t^c	Charging power per time step t [kW]
P_t^d	Discharging power per time step t [kW]
Q	Reactive power [VAr]
R	Battery investment/capital cost [\$]
S	Apparent power [VA]
SOC^t	State of charge per time step t [%]
SOH_t	State of health in time step t [%]

t	Time [minutes]
V	Voltage magnitude [V]
x	Variable [-]
Y	Admittance [S]
Y_{bus}	Bus admittance matrix [-]
y	Line admittance [S]
z	Line impedance [Ω]

List of Figures

- 2.1 Overview of the three levels in the Norwegian power system. 4
- 2.2 An illustration of a centralized power system. 5
- 2.3 An illustration of a decentralized power system. 6
- 2.4 Methods of demand response. 6
- 2.5 Magnitude/duration plot for voltage issues. 7
- 2.6 Flexibility resource characteristics. 8
- 2.7 Illustration of the most common quantitative attributes for flexibility resources. 9
- 2.8 Overview of the framework for a local flexibility market. 11
- 2.9 Areas of use for BESS in the distribution system. 12
- 2.10 The relationship between active-, reactive- and apparent power. 18
- 2.11 Newton-Raphson flow chart. 20
- 2.12 Illustration of two-stage stochastic optimization. 21
- 3.1 Single-line diagram of the case study network. 22
- 3.2 Active power load per radial. Based on [53]. 23
- 3.3 Placement of the battery in the case study. 24
- 4.1 Time series simulation module overview. 26
- 4.2 European Low Voltage Test Feeder network overview. 26
- 4.3 Cost of flexibility in cost profile 2. 37
- 4.4 Degradation cost per battery segment. 38
- 5.1 Voltage magnitude profiles for all buses for each load profile scenario. 40
- 5.2 Voltage magnitude profiles for load buses violating the under-voltage limit of 0.9 pu 41
- 5.3 Voltage magnitude profiles for load buses violating the power-quality limit of 0.95 pu 43
- 5.4 Flexibility demands for each load profile scenario as result of the two voltage limits, under-voltage and power quality. 44
- 5.5 Booking and activation of LongFlex and activation of ShortFlex using cost of flexibility profile 1. 45
- 5.6 Booking and activation of LongFlex and activation of ShortFlex using cost of flexibility profile 2. 46
- 5.7 Flexibility demand and second stage battery discharge for each flexibility demand scenario for the various cost profiles. 47
- 5.8 Second stage battery SOC for each cost profile. 48
- 5.9 Second stage battery segment SOC for cost of flexibility profile 1. 50
- 5.10 Second stage battery segment SOC for cost of flexibility profile 2. 51

List of Tables

- 2.1 Approaches and main findings from various references modelling battery degradation in optimization. 16
- 2.2 Bus classification. 17
- 4.1 Required input parameters for modelling bus elements in *PandaPower*. 27
- 4.2 Required input parameters for modelling single-phase line elements in *PandaPower*. 28
- 4.3 Required input parameters for modelling load elements in *PandaPower*. 28
- 4.4 Required input parameters for modelling a two-winding transformer element in *PandaPower*. 29
- 4.5 Required input parameters for modelling an external grid element in *PandaPower*. 29
- 4.6 Relevant results available from *PandaPower*. 30
- 4.7 The sets in the optimization model and their respective data. 35
- 4.8 The probability of each load profile/flexibility demand scenario. 36
- 4.9 Cost of flexibility profile 1. 37
- 4.10 Battery specifications for the case study battery. 38
- 4.11 Parameters used for battery degradation. 38
- 5.1 Distribution system operator costs per cost of flexibility profile. 52
- A.1 Presentation of line connections, line lengths and line types. i
- A.2 Presentation of the line type specifications. iii
- A.3 Transformer specifications. iii

Chapter 1

Introduction

This chapter firstly presents the background and motivation for this master thesis. Further, it presents a description of the scope of work and the contribution of this master thesis. Lastly, an outline of the master thesis is presented.

1.1 Background and Motivation

Due to the ongoing environmental issues there is an increase demand for renewable and more efficient energy generation. The power system is therefore transforming into a more decentralized system with a increased implementation of renewable energy sources, such as solar- and wind power, and more distributed generation. The reduction in pollution from power generation is important and necessary, however, the transformation of the power system, with more power generation in the distribution grid, causes issues for the distribution system operator, as the distribution system is not designed for connections with power generation [1][2][3].

The transformation causes among other, voltage related issues in the distribution grid and as the distribution system operator is responsible for maintaining the voltage quality within statutory limits, voltage control at distribution level is necessary [4]. There are many methods for voltage control in the distribution grid, however, in grids with a high penetration of renewable energy generation, the use of battery energy storage systems offers a reliable source for energy. Battery energy storage systems offers many areas of use in the distribution system such as voltage support [5][6]. However, the distribution system operator is not allowed to own, develop, manage or operate battery energy storage system as state by the current regulation from the European Commission [7]. However, the flexibility in batteries can be accessed through local flexibility markets [5].

This master thesis therefore focuses on the possibility of accessing the flexibility in batteries through local flexibility markets, and to evaluate the costs for the distribution system operator to do this considering the load uncertainty, the cost of booking and activating flexibility from a local flexibility market and how the cost of battery degradation might impact the total cost.

1.2 Scope of Work

This master thesis investigates the potential for using local flexibility markets as a way for the distribution system operator to access flexibility in battery energy storage systems for voltage control. This master therefore looks into the concept of flexibility, local flexibility markets, the areas of use for battery energy storage in the distribution grid and battery degradation. The scope of work can therefore be summarized to:

- **Voltage:** Presenting methods of voltage control in the distribution grid, voltage quality regulations and defining under-voltage issues.
- **Flexibility:** Describing the concept of flexibility, flexibility sources and the purpose of flexibility in the power grid. Presenting the framework for local flexibility markets as local flexibility markets and existing platforms.
- **Battery:** Investigate the area of use for battery energy storage in the distribution system and present methods for modelling battery degradation in optimization models.
- **Network modeling:** Modeling and simulating a realistic distribution grid using Norwegian load data to investigate under-voltage issues. Evaluate the demand for flexibility consider statutory voltage limits and power quality.
- **Two-stage optimization model:** Model a two-stage optimization model considering the load uncertainty, and investigate the total cost for the distribution system operator to book and activate flexibility through a local flexibility market and the effect of battery degradation on this cost. Evaluate the results of using various cost profiles for flexibility.

1.3 Contribution

This master thesis has several contributions such as an introduction to important concepts regarding the future power grid, such as flexibility, local flexibility markets and BESS in the distribution system. Another contribution is a review regarding battery degradation in optimization modeling. However, the two main contributions are presented below:

Network Model: One contribution of this master thesis is the model of the low voltage distribution grid in *PandaPower*. The model offers a network with common configurations of a low voltage distribution grid and load data from a distribution grid in Norway. The results from the simulations offers a network with violations of statutory levels and under-voltage issues.

Optimization Model: Another contribution is the two-stage stochastic optimization model in *Pyomo*. The optimization model considers the cost for DSO to procure flexibility, both long- and short term, through BESS, as well as the cost of battery degradation under the uncertainty of load with various cost profiles.

1.4 Thesis Outline

This report consists of six chapters:

Chapter 1: Introduction presents the background and motivation for the master thesis. Further, the scope of work and the contribution are presented. Lastly, an outline of the master thesis is presented.

Chapter 2: Theoretical Background** presents the necessary theoretical background for this master thesis. Firstly, it presents theory related to the distribution grid and the distribution grid operator, such as the decentralization of the power system, power quality regulation, under-voltage issues and voltage control. Further, the concepts of flexibility and local flexibility markets are described and the role of flexibility in the power system. The purpose of battery energy storage system in distribution grid is presented with methods for considering battery degradation in optimization modeling. Lastly, power flow analysis and stochastic programming are presented.

Chapter 3: Case Study presents the case study low voltage distribution grid used in the master thesis. It also presents three load profile scenarios and a battery case evaluated in combination with the case study network.

Chapter 4: Methodology** presents the modeling and simulation of the case study network with an explanation of the modelling process, necessary data, approaches to data handling and quasi-dynamic simulation. Further, the two-stage stochastic optimization model is presented and explained, as well as any assumptions and data used.

Chapter 5: Results and Discussion presents the results from both the network model and the two-stage stochastic optimization model in combination with a discussion of the results.

Chapter 6: Conclusion summarizes and concludes the report, and presents the main discoveries. It also presents thoughts around further work.

*** Note that some information presented in the specialization project “Reducing Voltage Related Challenges Through Flexibility and Modelling of a Distribution Grid” is re-used and re-written, for chapter 2 and 4, see reference [8].*

Chapter 2

Theoretical Background

This chapter presents the relevant theoretical background for this master thesis. Firstly, theory regarding the distribution grid, such as power quality regulation, decentralization of the power system, voltage issues and voltage control are presented. Further, the concept of flexibility and its role in the power system are presented, as well as the framework for local flexibility markets. Then the role of battery energy storage in the distribution grid and battery degradation are presented. Lastly, there is a presentation of power flow analysis and stochastic programming.

2.1 Distribution Grid

The Norwegian power system is divided into three levels; transmission-, regional distribution- and local distribution grid. Figure 2.1 presents an overview of the power system, differentiating the various levels. The transmission grid is a nationwide network binding together producers and consumers, as well as international connections, through a high voltage system, mostly at 300 kV or 420 kV [9][10].

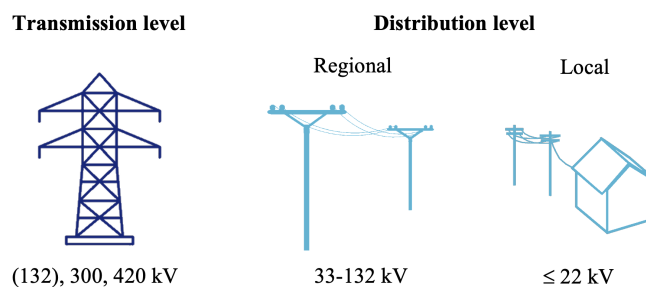


Figure 2.1: Overview of the three levels in the Norwegian power system. Based on [11, p.2].

According to European Union (EU) regulations, both regional- and local distribution grids are a part of the distribution system in Norway. However, the regional distribution grid is mainly used to bind together the transmission- and local distribution grid at a voltage level between 33-132 kV. The local part of the distribution system are the local grids, owned and operated by various grid companies, delivering power to smaller end-users. The local distribution grid is divided into a high voltage (HV) level, between 1-22 kV, and a low voltage (LV) level, at 230 V or 400 V, connected to end-users [9][10].

2.1.1 Power Quality Regulation

The distribution system operator (DSO) is responsible for operating and maintaining the distribution grid. In Norway there are over 100 DSOs responsible for the distribution grid in various areas of the country. The distribution of electrical power is a monopoly and the DSOs are therefore subjected to comprehensive regulations by the *energy law*. The regulations in the *energy law* are related to power production, sale, transfer, distribution and more [10][12][13].

Further, the *power quality regulation*, set by the Norwegian Water Resources and Energy Directorate (NVE), ensures that satisfactory power quality is delivered in the power system. The quality of delivered power is important as reduced quality might lead to consequences such as equipment failure and financial losses [4][14]. An important factor in delivered quality, is the voltage quality. The DSOs are responsible for ensuring that the slow variations in the voltage magnitude is within statutory limits. These limits are within the range of $\pm 10\%$ of the nominal voltage, measured as the average value over a minute, in connection with the LV-side of the local distribution grid [4].

2.1.2 From a Centralized to a Decentralized Power System

In a centralized power system the power generation is centralized at large-scale facilities, and these facilities are located far from the end-users. The power is transferred through the transmission grid and distributed to the end-users through the distribution grid [15]. Figure 2.2 presents an illustration of a centralized power system. However, due to environmental issues and the depletion of energy resources, there is an ongoing transformation of the power system. The demand for a decarbonized, renewable and more efficient energy generation challenges the traditional centralized management of the power system [1][2][3].

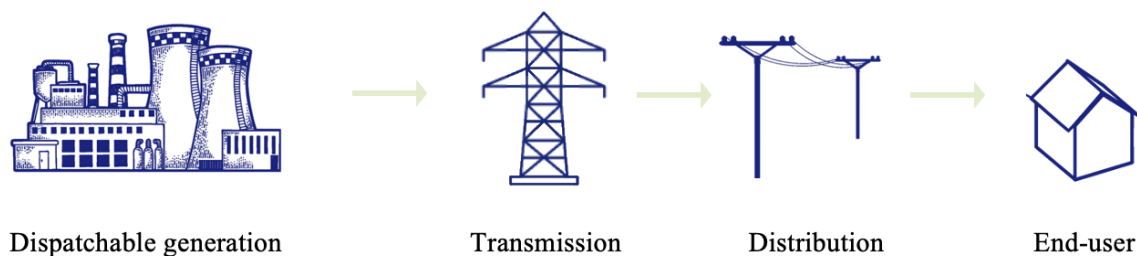


Figure 2.2: An illustration of a centralized power system. Based on [1].

The power system is therefore becoming more decentralized and more complex than a traditional centralized power system. An illustration of a decentralized power system is presented in figure 2.3. In a decentralized power system, the power generation comes from intermittent generation, such as solar- and wind power, and distributed generation (DG), in addition to large-scale facilities [1]. DG is a term used for a variety of power generation technologies connected to the distribution network. For the residential sector DG is technologies such Photovoltaic (PV) panels, backup generators and small wind turbines. These technologies might also be used in a bigger scale in the industrial and commercial sector, in addition to hydro power, combined heat and power (CHP) systems and more [16].

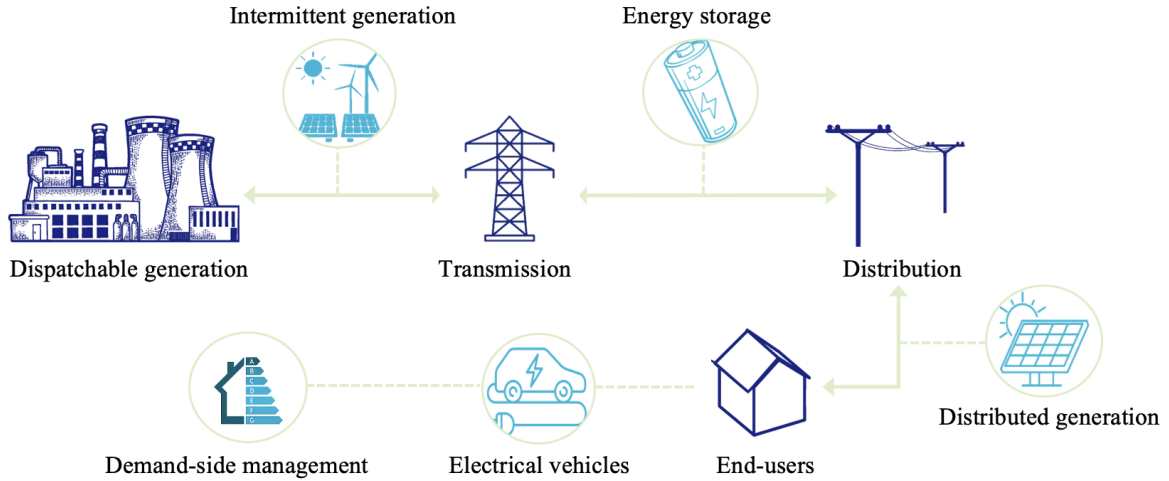


Figure 2.3: An illustration of a decentralized power system. Based on [1].

The increase in intermittent renewable energy sources (RESs) results in a need for energy storage systems (ESSs) to contribute towards a more reliable and efficient power system. There are several technologies for energy storage such as battery energy storage (BES), compressed air energy storage (CAES) and hydrogen energy storage (HES). Surplus energy generation can be stored in an ESS and be utilized during high demand to reduce the strain on the grid [17][18]. Further, an expectation in a decentralized power system is bi-directional power flow as a result of the consumers transitioning into prosumers. A prosumer is an end-user with their own power generation to cover some of their own demand. In periods with a power surplus, the end-user can sell power to the grid [19][20].

Demand-side management (DSM) is the implementation of various measures, such as demand response (DR), that can be utilized to improve the consumption-side of the power system [21]. DR is the end-users change of consumption pattern as a result of changes to the electricity price over time. The changes of consumption can be total consumption of electricity, timing and instantaneous demand. Figure 2.4 presents four methods of DR. The peak clipping technique is reducing the demand during peak hours without shifting the demand to off-peak hours. Shifting demand from peak hours to off-peak hours is load shifting. Valley filling is about increasing the off-peak hours load and flexible load shifting refers to increasing the consumption [22][23].

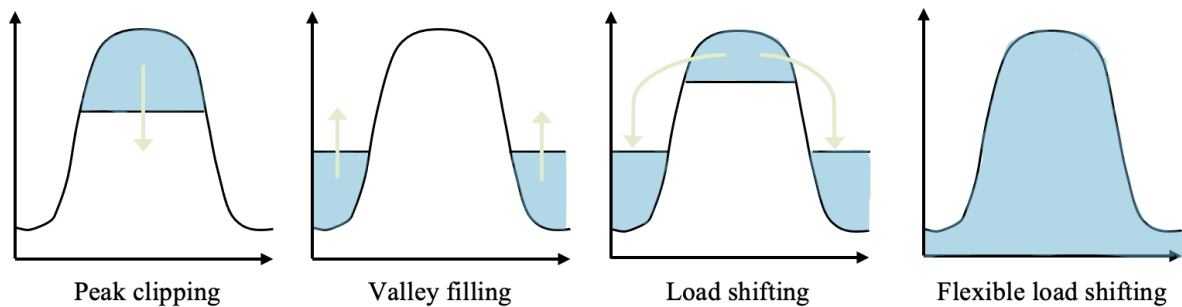


Figure 2.4: Methods of demand response. Based on [24].

2.1.3 Power Quality Challenges

The distribution system is not design for connections with power generation technologies and bi-directional power flow [25]. The ongoing transformation of the power system therefore results in voltage related challenges in the distribution system. Voltage issues can be defined by the voltage magnitude and the duration of the event, as presented in figure 2.5. Voltage magnitude issues can be split into; interruption, over- and under voltage [26]. This master thesis focuses on long and very long under-voltage issues.

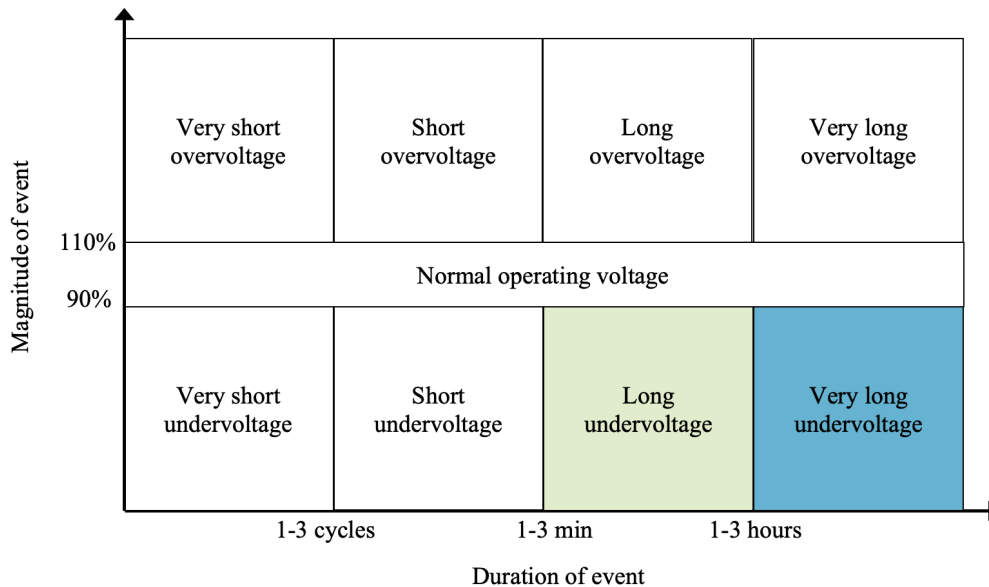


Figure 2.5: Magnitude/duration plot for voltage issues. Based on [26, p.8].

Long-Duration Voltage Variations

Long-duration voltage variations are deviations from the nominal voltage for more than one minute, and are classified as under-voltage when the nominal voltage is between 0.8-0.9 pu [26]. In a local distribution system with a nominal voltage at 230 V, under-voltage is below 207 V. Under-voltage issues are created when the voltage drops too low as a result of a great load, meaning that the distribution system is too weak to handle the load [27].

2.1.4 Voltage Control in the Distribution System

In traditional distribution grids voltage control is usually done by conventional volt/VAr control (VVC) devices, such as on-load tap changer (OLTC) and step voltage regulator (SVR). An OLTC is a transformer component used to automatically change the tap position and thereby creating an increase or decrease in voltage at the substation. If the voltage level is outside of a set perimeter the OLTC is activated. In a centralized control strategy the high penetration of DG and distributed energy resources (DERs) in the distribution grid results in a high variation in voltage levels throughout the day resulting in many tap variations. Frequent use of the OLTC under load results in material degradation, which impacts the lifespan of the component. To provide efficient voltage control the OLTC can be used in combination with other reactive power control devices, such as the static var compensator (SVC) or shunt capacitor (SC) [28][29][30].

In automatic voltage regulating (AVR) systems the OLTC is used in combination with a SC at the primary substation for voltage control by adjusting the reactive power output. This would be enough voltage regulation in a traditional distribution grid. Further, the SVR is operated like the OLTC, but it is used for feeder-level control and is therefore installed in each feeder and not at the substation. Thereby providing voltage regulation which improves the voltage profile of the transmission line [5] [28].

The methods presented above are traditional methods of voltage control, however, in a grid with a high penetration of renewable generation the use of battery energy storage provides a reliable energy source. ESS can be used for voltage control in the distribution grid as it could be used to reduce the difference between supply and demand. In a distribution system the use of ESS would result in voltage support, security of supply, reduced power loss and a reduced need for grid reinforcement [5]. This master thesis focuses on voltage control by the use of ESS to procure flexibility to reduce under-voltage issues and maintaining power quality.

2.2 Flexibility

Flexibility is defined as the possibility of modifying the generation and consumption patterns in reaction to a signal. Flexibility is further defined as the power system networks capacity and ability to sustain reliable supply during imbalance between supply and demand [31].

2.2.1 Flexibility Resources

A flexibility resource is a resource with the ability of flexibility, meaning the ability to respond to a request in services such as time, availability, volume and cost. In [32] the characteristics of flexibility resources are divided into two main groups, technical- and economic characteristics, with sub-classifications. This is presented in figure 2.6.

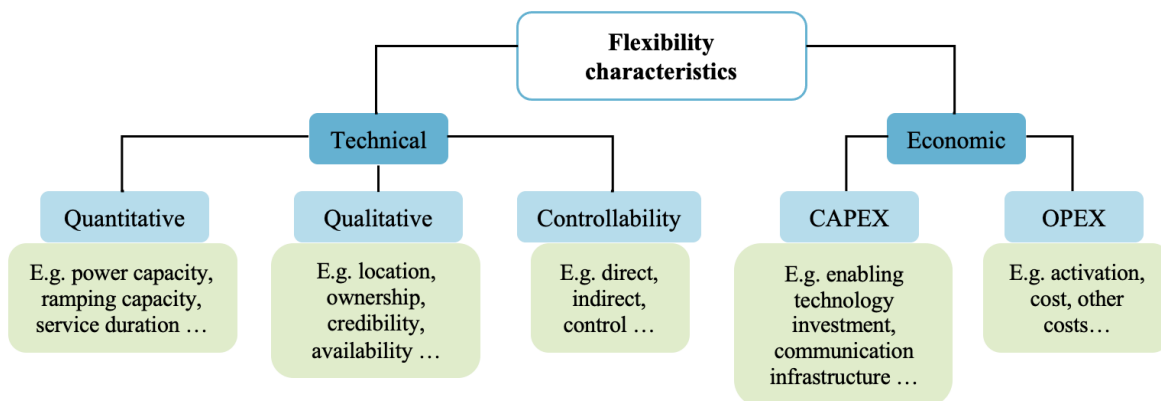


Figure 2.6: Flexibility resource characteristics. Based on [32].

The economic characteristics are classified into capital (investment) expenditure characteristics (CAPEX) and operational expenditure characteristics (OPEX). CAPEX refers to the investment cost of the flexibility resources and enabling activation of flexibility, while OPEX focuses on the other cost related to activation of flexibility and aging as a result of activation [32].

The technical characteristics are classified into three groups; qualitative, controllability and quantitative. The qualitative technical characteristics refer to the flexibility resources quality expressed as a degree of comparison and the control technical characteristic refers to how the flexibility resources are controlled. The quantitative technical characteristics refer to the numerically expressed capability of flexibility resources [32].

In [2] and [3] the most commonly used attributes to characterize flexibility resources, that falls within quantitative- and qualitative technical characteristics, are stated as;

- Direction
- Power capacity (power modulation)
- Ramping capacity (rate of change, gradient)
- Service duration
- Location

In [2], [3] and [32] these attributes are defined similarly, however, using various terms for the same attribute. Location is a qualitative technical characterization states the location of the flexibility resource in the system. Direction, power capacity, ramping capacity and service duration are quantitative technical characterizations. Direction is stated as $+/-$ a numerical value referring to an increase or decrease in net power output, as flexibility can be provided in both direction by some flexibility resources.

Power capacity or power modulation, in MW or MVar, is stated as the capability of delivering a change in power output. The ramping capacity, in MW/s, is defined as rate of change or the gradient, meaning the maximum change in power output as a function of time. Further, service duration, in seconds, refers to how long the flexibility resource can provide flexibility [2][3][32]. These quantitative attributes are illustrated in figure 2.7.

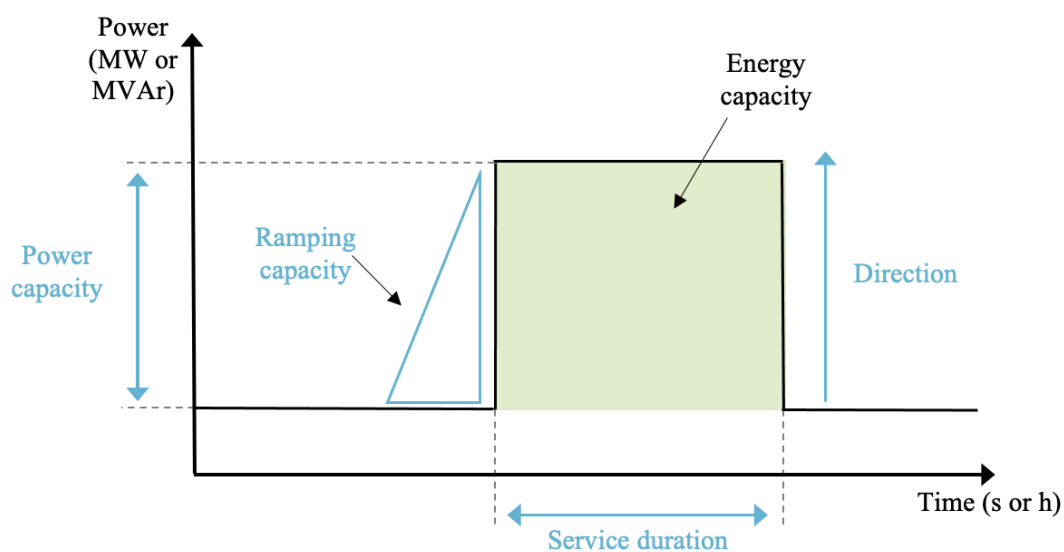


Figure 2.7: Illustration of the most common quantitative attributes for flexibility resources. Based on [32] and [33, p.239].

2.2.2 Distribution System Flexibility

In power systems with a high penetration of renewable energy generation, there is a need for increased flexibility for both planning and operation of the power system. The access to flexibility will be important in the evolution of modern power systems as it will allow for more effective renewable integration in the power system [31]. Reference [34] presents two main purposes of flexibility in the power system, as presented below.

- **Transmission Level:** Mitigate the imbalance between supply and demand
- **Distribution Level:** Reduce overloading and the violation of statutory voltage limits

In [3] flexibility is classified into three types of products depending on purpose. These types and purposes are presented below.

- **Type 1:** Balancing flexibility for the transmission system operator (TSO) at transmission level available through e.g. the intra-day energy market.
- **Type 2:** Balancing flexibility for TSO at distribution level available through DERs at distribution level.
- **Type 3:** Flexibility for DSO at distribution level to be used for congestion management, voltage control and reduction of losses.

This master thesis focuses on the flexibility in the distribution grid, more specifically type 3 flexibility. In [3] type 3 flexibility is divided into three sources of flexibility dependent on where in the distribution grid the flexibility is available.

- **Grid-side flexibility:** Grid-side flexibility refers to the flexibility available through various grid equipment; discrete equipment such as OLTC and remotely controllable switches (RCSs), and controllable power electronic devices such as soft open point (SOP). The equipment can be used to improve the operation of the system and thereby offering flexibility.
- **Supply-side flexibility:** Coordinated operation of DGs, such as diesel generator, fuel cell, BESS and CHP plant, leads to flexibility at the supply-side.
- **Demand-side flexibility:** Demands-side flexibility refers to the flexibility created by the end-users. This can be achieved through DSM, heat pumps, electrical vehicles (EVs) and heating, ventilation and air conditioning (HVAC) systems.

2.2.3 Local Flexibility Market

A local flexibility market (LFM) is an electricity trading platform to buy and sell flexibility within limited geographical areas. Local flexibility markets presents one solution for procuring flexibility in the distribution system [2][3].

Framework

There are several key participants in a local flexibility market, and the participants have various objectives and roles [3]. The key participants in a local flexibility market are generally:

- Balance responsible party
- Distribution system operator
- Aggregator
- Local flexibility market operator

The buyers in the LFM are the DSO and the balance responsible party (BRP). The BRP is a trader in the electricity market outsourced by clients, which is responsible for the energy balance between supply and demand, and is therefore interested in procuring flexibility to ensure that balance. The DSO also has an interest in acquiring flexibility for various operation functions, such as voltage control and congestion management [3].

The flexibility in the LFM is provided by various generation asset owners, such as prosumers, and ESS operators. However, as they individually have a limited amount of flexibility and therefore hold little negotiation power on their own in the market, an aggregator gathers these individual flexibility providers and trades on their behalf. The local flexibility market operator provides a trading platform and supervises the trading between the market participants [3]. Figure 2.8 presents an overview of the LFM framework.

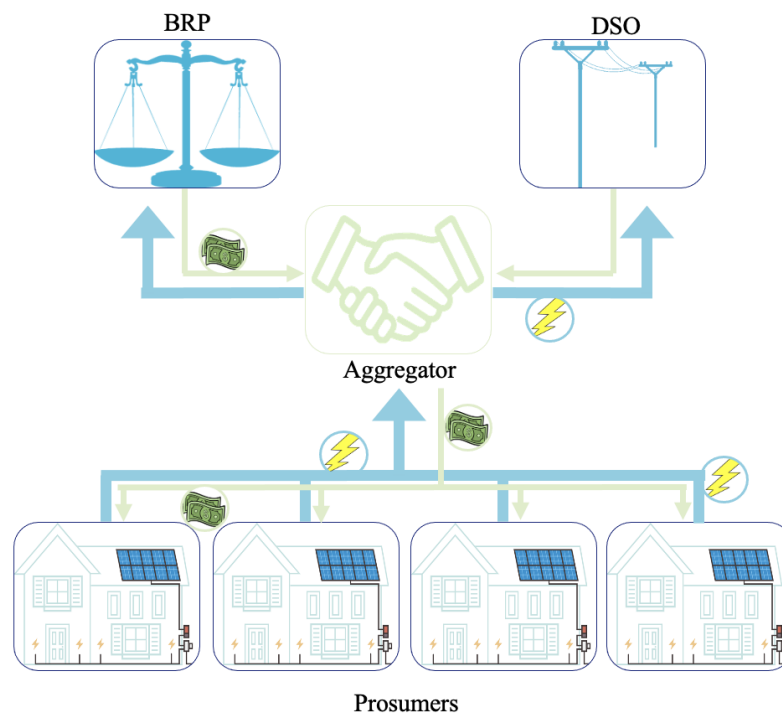


Figure 2.8: Overview of the framework for a local flexibility market. Based on [35].

2.2.4 NODES

NODES is an independent market operator offering flexibility in the grid through an open marketplace for flexibility providers and grid operators. NODES operates in Norway, Sweden and the UK, securing the supply of flexibility for various participants in the power system. NODES offers selling and buying of flexibility through two various platforms; ShortFlex and LongFlex [36].

- **ShortFlex:** Close to real-time flexibility trade in a continuous market, with a price of buying/activation [37].
- **LongFlex:** Contracts for booking flexibility a head of time to ensure available flexibility for the DSO. LongFlex consist of an availability/booking price and an activation price [38].

2.3 Battery Energy Storage Systems

The development of the technology and cost of batteries have made battery energy storage systems (BESS) a good alternative to traditional grid investments. There are several areas of use for BESS in a distribution system, which can be divided within security of supply, security of delivery and power equalization [6]. Figure 2.9 presents the area of use for BESS in the distribution system. This master thesis focuses on the use of BESS for voltage support in the distribution system.

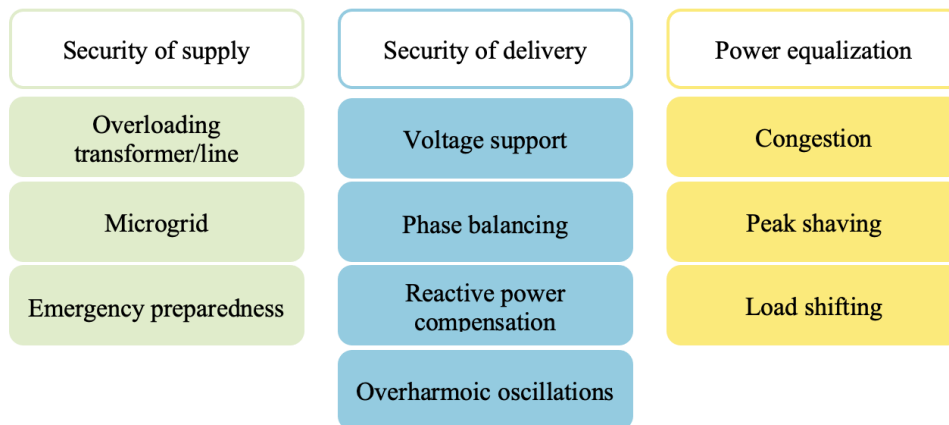


Figure 2.9: Areas of use for BESS in the distribution system. Based on [39, p.17]

2.3.1 BESS in Distribution Systems

BESS is suitable for handling under-voltage issues as it can be used to rapidly adjust the active- and reactive power generation in the system, and thereby regulating the voltage quality of the system [40]. Voltage related challenges in the distribution system are local problems, which are therefore required to be solved locally [6]. One advantage to BESS is the independence to geographical factors, and the BESS can therefore be placed close to the demand for voltage support in the grid [40]. BESS can therefore also be used to postpone infrastructure upgrades [18], and as batteries are flexible, meaning batteries can easily be disassembled and moved, if the load situation changes or upgrades of the infrastructure are to be made [6].

Ownership

One of the main advantages considering the DSO owning BESS is full control over capacity and availability [6]. However, current regulations from the European Commission states that DSOs are not allowed to own, develop, manage or operate BESS [7]. Therefore, other options of access to BESS in distribution systems have to be considered. Another option for BESS access is through LFM [5].

2.3.2 Characteristics

There are many types of batteries, however, compared to other types of batteries, lithium-ion batteries have a high power density and cycle life. This makes lithium-ion batteries a good candidate for grid application. Additionally, the cost of lithium-ion batteries are decreasing and is expected to continue to decrease [41]. There are several battery parameters that are used to characterize a battery, and some important battery characteristics are presented below [42].

- **Energy capacity** is the amount of energy that can be stored in the battery in kWh
- **Maximum charging/discharging** is the maximum rate of charging/discharging in a given instance in kW
- **Roundtrip efficiency** is an indicator for the percentage of energy going into the battery that might be withdrawn
- **State of Charge (SOC)** refers to the level of charge in the battery
- **State of Health (SOH)** describes the difference in state between a new battery and the studied battery
- **Depth of Discharge (DOD)** is a percentage of the total capacity discharged
- **Cycles** is a measure of the battery lifetime for a given DOD

2.3.3 Stress Factors in Battery Degradation

Batteries experience degradation over time which is influenced by various stress factors. The effects of battery degradation that can be observed are capacity- and power fade, the reduction in usable capacity and delivered power [40]. Several of this stress factors are presented below.

- **Cycle aging** occurs as result of charging and discharging cycles causing fading of active materials. Batteries have a limited cycle life, and more frequent cycling increases the battery cell degradation [40].
- **High/low SOC** levels as a result of over charging and discharging, reduces the battery lifetime [40][43].
- **Cycle depth**, or DOD, is an important factor as deeper cycles reduces a battery's amount of possible cycles and lifetime [43]
- **Calendar aging** refers to battery degradation as a result of time without external influence [40]
- **Ambient temperature** is the air temperature at the battery [44]

2.3.4 Modeling of Battery Degradation in Optimization

This section investigating various methods of modelling battery degradation and battery degradation cost in optimization modelling. The focus is therefore on the equations and approaches used for battery degradation, and not the full optimization models.

In reference [45] the cost of battery degradation is measured as the cost of degradation per kWh and the cost of degradation per cycle. The degradation cost in \$/kWh, B , is presented in equation 2.1a, where R is the investment cost in \$, L is the lifetime throughput in kWh and E is the squareroot of the roundtrip efficiency. The degradation cost per cycle in \$, B_c^n , is presented in equation 2.1b, where index n is the depth of discharge as a fraction of the capital cost in \$, R , and the remaining cycles to failure f_n .

$$B = \frac{R}{L \cdot E} \quad (2.1a)$$

$$B_c^n = \frac{R}{f_n} \quad (2.1b)$$

Reference [43] has established a marginal cost function reflecting the cost of battery degradation caused by cycles. The piecewise linear upper-approximation function for cost, c , as a function of the cycle depth, δ_t , is presented in equation 2.2. The equation considers the battery replacement cost in \$, R , the battery discharge efficiency in %, η_{dis} , the battery energy capacity in \$/kWh, E^{rate} , the total amount of battery segments J , the current battery segment j and loss of life per cycle in %, Φ . The marginal cost function was used in an optimization model to optimize the BESS dispatch.

$$c(\delta_t) = \begin{cases} c_1 & \text{if } \delta_t \in [0, \frac{1}{J}) \\ \vdots & \\ c_j & \text{if } \delta_t \in [\frac{j-1}{J}, \frac{j}{J}) \\ \vdots & \\ c_J & \text{if } \delta_t \in [\frac{J-1}{J}, 1] \end{cases}$$

where

$$c_j = \frac{R}{\eta^{dis} E^{rate}} J \left[\Phi \left(\frac{j}{J} \right) - \Phi \left(\frac{j-1}{J} \right) \right] \quad (2.2)$$

The marginal cost function established in reference [43] gives a close approximation the actual cycle aging of electrochemical batteries. Reference [46] has implemented this function into a two-stage stochastic model considering flexibility booking for congestion management as well as battery degradation.

In reference [44] the cost of battery degradation is implemented into a optimal operational scheduling of a virtual power plant by the use of several equations. Equation 2.3a calculates the DOD for every time step t , where SOC^t is the SOC in time step t and E_{BESS}^{max} is the maximum energy stored in the BESS in MWh. Equation 2.3b states the relation between the DOD and the battery cycle life L_{DOD} , in cycles, where a and b are cycle life coefficients dependent on DOD. Equation 2.3c states the relationship between the ambient temperature in °C, T , and the number of cycles, L_{temp} , where m and ϕ are cycle life coefficients dependent on the ambient temperature.

$$DOD^t = 1 - \frac{SOC^t}{E_{BESS}^{max}} \quad (2.3a)$$

$$L_{DOD} = a \cdot DOD + b \quad (2.3b)$$

$$L_{temp} = m^{\phi T} \quad (2.3c)$$

$$L_{VVP} = \frac{L_{DOD} \cdot L_{temp}}{L_R} \quad (2.3d)$$

Equation 2.3d combines the effect of ambient temperature and DOD to calculate the cycle life of the battery with VPP (virtual power plant) participation, L_{VPP} , where L_R is the rated cycle life of the battery by the producer. The cost of battery degradation, C_{BD} , is then calculated by considering the DOD and the ambient temperature, as presented in equation 2.4. C_{BC} is the captial cost of the battery and E^{total} is the total energy storage in the battery [44].

$$C_{BD} = \frac{C_{BC} \cdot L_R}{L_{DOD} \cdot L_{temp} \cdot E^{total} \cdot DOD^{ref}} \quad (2.4)$$

Reference [47] implements the battery degradation in an optimization model for a battery energy storage system EV fast charging station, by the use of the equations presented below. Equation 2.5a states that the actual energy at all times in kWh, $E^{B,cap}$, is obtained from multiplying SOH in every time step t in %, SOH_t , with the initial battery capacity in kWh, E^{B0} . In equation 2.5b the SOH_t is calculated by dividing the energy stored, E_t^B , by the battery capacity, $E^{B,cap}$. Equation 2.5c states that the C-rate, speed to full charge/discharge, C_t^r is obtained by the power discharged from the BESS, P_t^B , by the initial battery capacity, E^{B0} .

$$E^{B,cap} = SOH_t \cdot E^{B0} \quad (2.5a)$$

$$SOC_t = \frac{E_t^B}{E^{B,cap}} \quad (2.5b)$$

$$C_t^r = \frac{P_t^B}{E^{B0}} \quad (2.5c)$$

Equation 2.6a states that the cyclic aging function, f_t^c , is obtained by the use the two cyclic aging factors, $\kappa_{C_{r0}}$ and $\kappa_{C_{r1}}$, and the C-rate, C_t^r . The full equivalent cycle FEC_t is obtained, in equation 2.6b, by multiplying the charging power, P_t^c , by the discharging power, P_t^d , and then dividing it by the difference between the minimum and the maximum SOC, $SOC_{max} - SOC_{min}$, multiplied with two times the E^{B0} . In equation 2.6c the calendar aging is stated as a temperature dependent factor, κ_K , multiplied with squareroot of time t , and the cyclic aging is stated by cyclic aging function, f_t^c , multiplied with the full equivalent cycle FEC_t . The SOH_t is then $SOH_t = \text{minus the calendar aging and cyclic aging [47]}$.

$$f_t^c = \kappa_{C_{r0}} + \kappa_{C_{r1}} \cdot C_t^r \tag{2.6a}$$

$$\Delta FEC_t = \frac{P_t^c \cdot P_t^d}{2E^{B0} \cdot (SOC_{max} - SOC_{min})} \tag{2.6b}$$

$$\Delta SOH_t = SOH_{t0} - \kappa_K \cdot \sqrt{t} - f_t^c \cdot FEC_t \tag{2.6c}$$

The main findings from the various references presenting the modelling of battery degradation and battery degradation costs in optimization are presented in table 2.1.

Table 2.1: Approaches and main findings from various references modelling battery degradation in optimization.

Ref	Approach	Main findings
[43]	Cycle aging, cost of degradation per segment	BES probability and life expectancy improved considering battery degradation
[44]	Cost of degradation based on DOD and ambient temperature	Battery degradation has an important effect on the profit and must be considered in maximum profit problems.
[45]	Cost of degradation per kWh, cost of degradation per cycle	The importance of taking the relationship between operation and degradation considering the economic operation of storage. Important for extending the life of the battery.
[46]	Cycle aging, battery segment cost based on cycle depth	Solving the same problem with and without considering degradation costs showed how important it is to account for the realistic cost of using the battery for flexibility
[47]	Calendar aging, cycle aging	Battery degradation has a minimal impact on the operation cost, but an impact on the investment costs. The dominant term in the battery degradation is the calendar aging.

2.4 Power Flow and Stochastic Programming

This sections presents the concept alternating current (AC) power flow analysis and its area of use. It also presents stochastic programming for optimization.

2.4.1 AC Power Flow Analysis

Power flow, also referred to as load flow, analysis is a numerical analysis of a power system operating under balanced and steady-state conditions. The power system consists of generators, loads and buses connected together by transmission lines. The analysis is done to obtain voltages, currents, powers and losses in the network. Thereby making power flow analysis a useful tool for planning, operation and economic scheduling of power systems. [48][49]

Bus Classification

It is necessary to begin the power flow analysis by classifying the buses in the power system to determine the specified and unknown variables. The buses are classified into; PQ bus, PV bus and slack bus, where each bus type has a set of specified and unknown variables. The bus types with their specified and unknown variables are presented in table 2.2 [48][49].

Table 2.2: Bus classification. Based on [49].

Bus type	Specified variables	Unknown variables
PQ / Load	P_i, Q_i	$\delta_i, V_i $
PV / Regulated	$P_i, V_i $	Q_i, δ_i
Slack / Reference	$\delta_i, V_i $	P_i, Q_i

The PQ bus is a load bus as both the active (P) - and reactive (Q) power is known. The power consumed in the system is defined as negative, while the power supplied to the system is defined as positive. The unknown variables for a PQ bus are the voltage magnitude ($|V|$) and voltage angle (δ) [48][49].

The PV bus is a voltage controlled bus as it is where the generator is connected, and it is controlled as the voltage magnitude is known. The active power is also specified, while the voltage angle and reactive power are unknown. The slack bus acts as the reference bus in the system. The voltage angle and magnitude are specified and assumed to be 0° and 1 pu, respectively, while the active- and reactive power are unknown. Further, the slack bus provides the difference between the scheduled loads and the power generation as a result of the losses in the system [48][49].

Bus Admittance Matrix

The bus admittance matrix, Y_{bus} , reduces a complex system into a matrix. The Y_{bus} can be obtained by examining the structure of the network and using the transmission line impedance, z . The dimension of the Y_{bus} -matrix is $N \times N$, where N is the number of buses in the system. The Y_{bus} -matrix is presented in equation 2.7 [50].

$$Y_{bus} = \begin{bmatrix} Y_{11} & Y_{12} & \dots & Y_{1i} & \dots & Y_{1n} \\ Y_{21} & Y_{22} & \dots & Y_{2i} & \dots & Y_{2n} \\ \dots & \dots & \dots & \dots & \dots & \dots \\ Y_{i1} & Y_{i2} & \dots & Y_{ii} & \dots & Y_{in} \\ \dots & \dots & \dots & \dots & \dots & \dots \\ Y_{n1} & Y_{n2} & \dots & Y_{ni} & \dots & Y_{nn} \end{bmatrix} \quad (2.7)$$

The line admittance, y_{ij} , between bus i and j is calculated by using equation 2.8, where z_{ij} is the transmission line impedance between bus i and j [50].

$$y_{ij} = \frac{1}{z_{ij}} \quad (2.8)$$

The off-diagonal elements, Y_{ij} , is equal to the negative line admittance calculated in equation 2.8. The diagonal elements, Y_{ii} , in the admittance matrix are the self-admittances, which is the sum of all line admittances, y_{ij} , connected to bus i . Equation 2.9 is used to calculate the self-admittance of bus i [50].

$$Y_{ii} = \sum_{j=0}^n y_{ij} \quad j \neq i \quad (2.9)$$

Power Flow Equations

The power in an AC power system is active power, reactive power or apparent power (S). The relationship between the active-, reactive- and apparent power and the phase angle (ϕ) are presented in figure 2.10 [50].

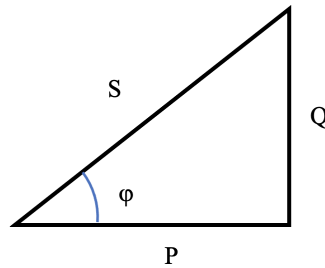


Figure 2.10: The relationship between active-, reactive- and apparent power. Based on [50, p.50].

The relationship between the active-, reactive- and apparent power results in equation 2.10. The apparent power, in VA, is the square root of the active power, in W, squared and the reactive power, in VAR, squared [50].

$$S = \sqrt{P^2 + Q^2} \quad (2.10)$$

The powerfactor, $\cos\phi$, is obtained from dividing the active power by the apparent power. This is presented in equation 2.11 [50].

$$\cos\phi = \frac{P}{S} \quad (2.11)$$

The use of power flow equations are required to analyze the power flow in the power system. The power flow equations for active- and reactive power presented in 2.12 and 2.13, respectively. Where i and j denote the bus number, Y is the bus admittance, $|V|$ is the voltage magnitude, θ is the phase angle and δ is the voltage angle [50].

$$P_i = \sum_{j=1}^n |Y_{ij}| |V_j| |V_i| \cdot \cos(\theta_{ij} - \delta_i + \delta_j) \quad (2.12)$$

$$Q_i = - \sum_{j=1}^n |Y_{ij}| |V_j| |V_i| \cdot \sin(\theta_{ij} - \delta_i + \delta_j) \quad (2.13)$$

Power Mismatch, Sensitivity and Unknowns

The jacobian matrix is a matrix of sensitivity and contains the power flow equations partially deviated by the voltage magnitude and angle. The jacobian matrix is presented in equation 2.14 [50].

$$J = \begin{bmatrix} J^1 & J^2 \\ J^3 & J^4 \end{bmatrix} = \begin{bmatrix} \frac{\partial P_i}{\partial \delta_i} & \frac{\partial P_i}{\partial |V_i|} \\ \frac{\partial Q_i}{\partial \delta_i} & \frac{\partial Q_i}{\partial |V_i|} \end{bmatrix} \quad (2.14)$$

Further, the power mismatch vector accounts for both the active- and reactive power at each bus. The power mismatch vector is the difference between the scheduled power and the calculated power for each bus, and this is presented in equation 2.15 [50].

$$\begin{bmatrix} \Delta P_i \\ \Delta Q_i \end{bmatrix} = \begin{bmatrix} P_i^{sch} \\ Q_i^{sch} \end{bmatrix} - \begin{bmatrix} P_i^{calc} \\ Q_i^{calc} \end{bmatrix} \quad (2.15)$$

The power mismatch vector is equal to the jacobian matrix multiplied with the vector of unknown voltage magnitudes and and angles, as presented in equation 2.16. The vector of unknown voltages can be obtain by multiplying the power mismatch vector by the inverse of the jacobian matrix [50].

$$\begin{bmatrix} \Delta P_i \\ \Delta Q_i \end{bmatrix} = \begin{bmatrix} \frac{\partial P_i}{\partial \delta_i} & \frac{\partial P_i}{\partial |V_i|} \\ \frac{\partial Q_i}{\partial \delta_i} & \frac{\partial Q_i}{\partial |V_i|} \end{bmatrix} \begin{bmatrix} \Delta \delta_i \\ \Delta |V_i| \end{bmatrix} \quad (2.16)$$

Newton-Raphson

The Newton-Raphson method is the most widely used method for solving simultaneous non-linear algebraic equations. The method is a successive approximation method using an initial estimate, x^k , of the unknown variables and Taylor series expansion. The next estimate, x^{k+1} , in the Newton-Raphson iteration is obtained by using in equation 2.17, where Δx^k is small deviation from the correct solution [49].

$$x^{k+1} = x^k + \Delta x^k \quad (2.17)$$

The Newton-Raphson method used for power flow analysis is presented by the flow chart in figure 2.11. The first step is to evaluate the data for the power system and set up the Y_{bus} . Then making an initial estimate of the voltages, e.g. assuming a flat start for each bus (0° and 1 pu). The next step is to calculate P^{calc} and Q^{calc} by using the power flow equations presented in equation 2.12 and 2.13 [50].

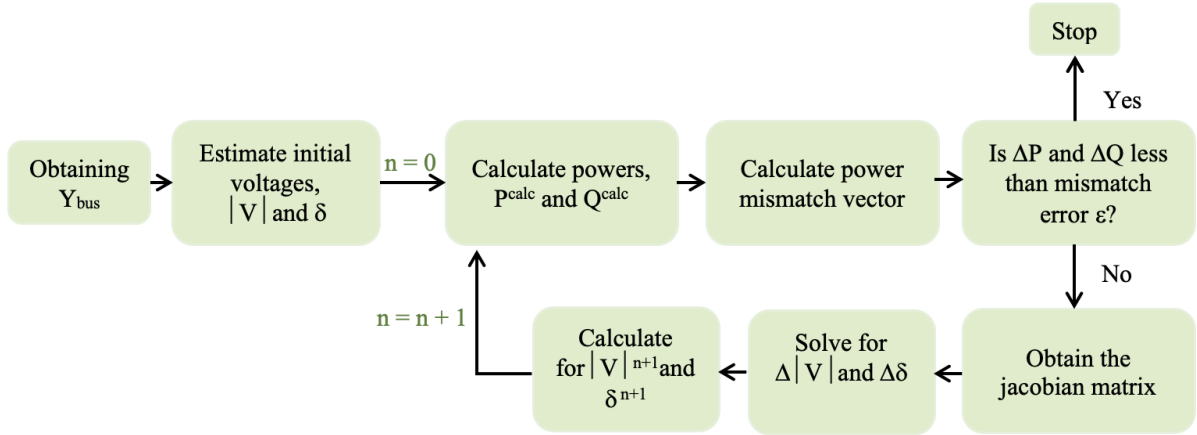


Figure 2.11: Newton-Raphson flow chart. Based on information from [50].

The power mismatch vector can then be calculated by equation 2.15. If the power mismatch is below a set mismatch error (ϵ) the power flow analysis is done, but if it is not, the jacobian matrix in equation 2.14 must be obtained. The vector of unknown voltages is then be calculated as presented in equation 2.18 [50].

$$\begin{bmatrix} (\Delta\delta_i)^n \\ (\Delta|V_i|)^n \end{bmatrix} = J^{-1} \begin{bmatrix} (\Delta P_i)^n \\ (\Delta Q_i)^n \end{bmatrix} \tag{2.18}$$

The last step is to calculate the voltage angles and magnitude for the next iteration. This is done by adding the initial voltage angles and magnitudes of the iteration with the voltages calculated in equation 2.18. This is presented in equation 2.19 [50].

$$\begin{bmatrix} (\delta_i)^{n+1} \\ (|V_i|)^{n+1} \end{bmatrix} = \begin{bmatrix} (\delta_i)^n \\ (|V_i|)^n \end{bmatrix} + \begin{bmatrix} (\Delta\delta_i)^n \\ (\Delta|V_i|)^n \end{bmatrix} \tag{2.19}$$

2.4.2 Stochastic Programming for Optimization

Stochastic programming, or stochastic optimization, is a method for making decisions under uncertainty. The uncertainty in the model is related to data used within the model. Thereby creating various scenarios of different variations of the data, where the scenarios represents different situations with various probability. The point of stochastic programming is to obtain the optimized goal of the model over all the scenarios, thereby accounting for the uncertainty of the scenarios [51].

Two-stage stochastic optimization is one case of stochastic programming. In the first stage the decisions are made “here and now”, meaning the decision is made based on the available data at that time. The first stage is followed by the realization of uncertainty. The second stage decisions are the “wait and see” decisions and are therefore corrective decisions [51]. Figure 2.12 presents an illustration of two-stage stochastic optimization.

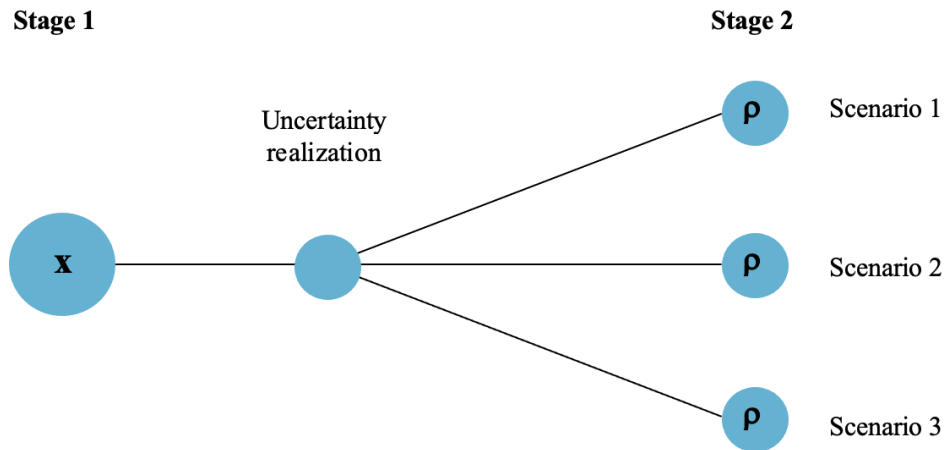


Figure 2.12: Illustration of two-stage stochastic optimization, where x is the first stage decision and ρ is the probability of each scenario [51].

Chapter 3

Case Study

This chapter presents an overview of the case study used in this master thesis. The case study network is a low voltage distribution grid based on the European Low Voltage Test Feeder from IEEE PES AMPS DSAS Test Feeder Working Group. The European Low Voltage Test Feeder represents a low voltage distribution system in Europe with common configurations of low voltage systems [52]. Further, three load profile scenarios and a battery case are presented.

3.1 Network Overview

Figure 3.1 presents a single-line diagram of the case study network. The case study network is a low voltage distribution grid connected to the HV-side of the distribution grid (external grid) by a transformer. The network is divided into three radials, consisting of a total of 50 buses, where 24 of them are load buses and the rest are measuring buses, marked as nodes in the single-line diagram.

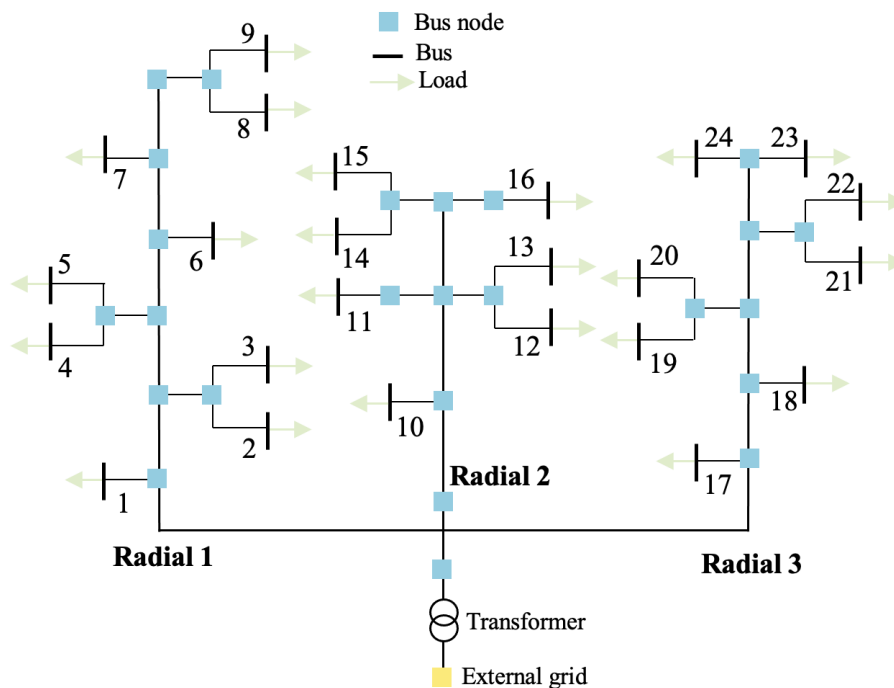
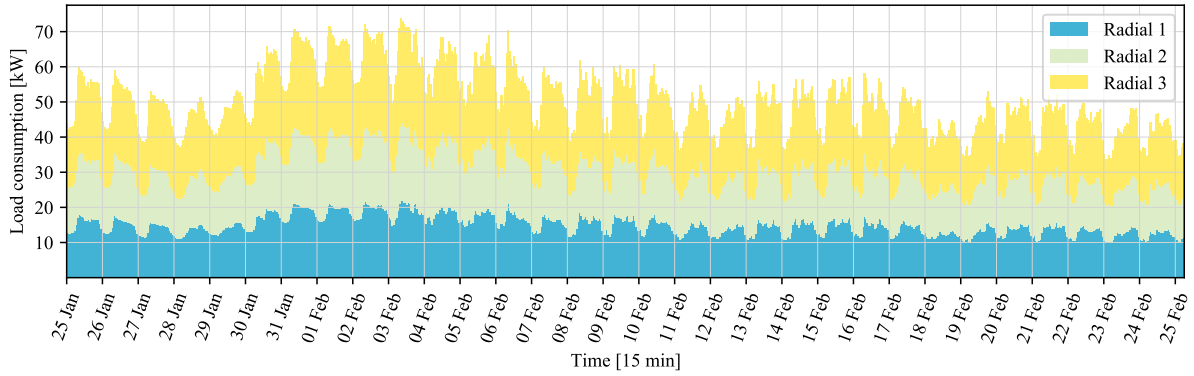


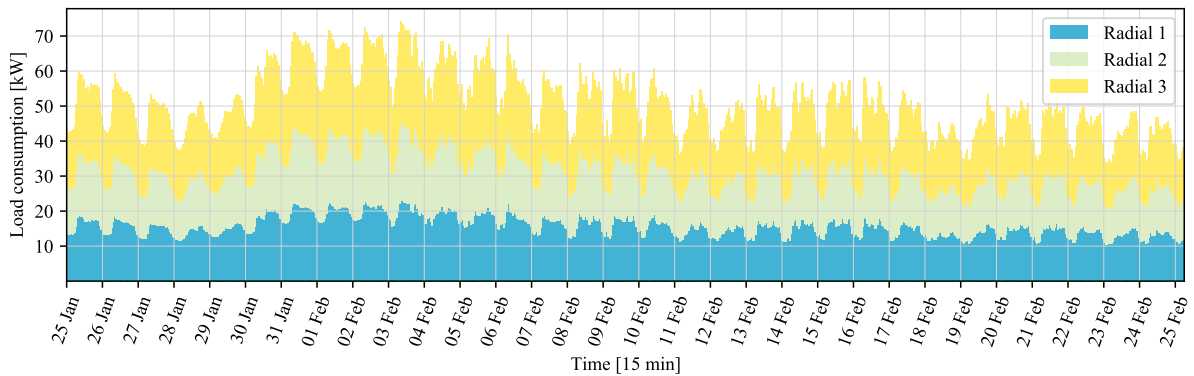
Figure 3.1: Single-line diagram of the case study network.

3.2 Load Profile Scenarios

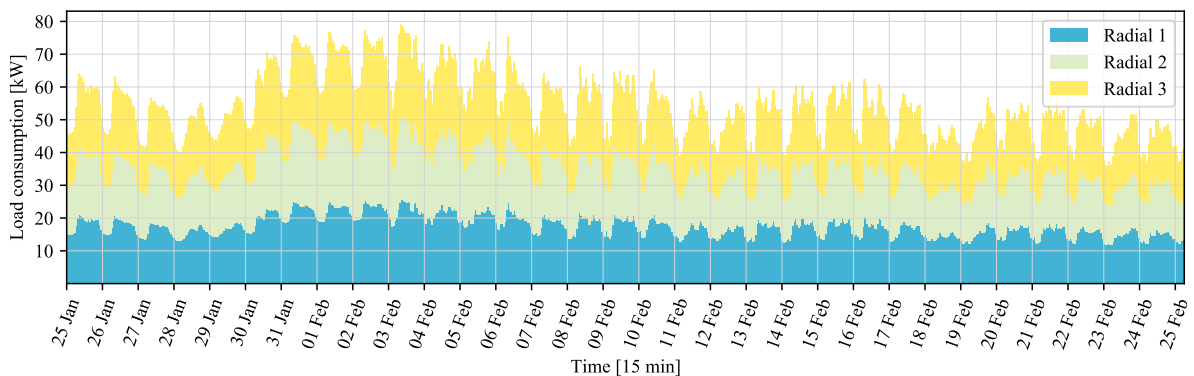
Three load profile scenarios were created for the case study using load data from a modified version of a distribution grid at Steinkjer, Norway [53]. The load profile scenarios are presented in 3.2. Load profile scenario 1 is presented in 3.2a, load profile scenario 2 is presented in 3.2b and load profile scenario 3 is presented in 3.2c. These figures present the load data from the 25.01.2012 to the 25.02.12 of the available data.



(a) Load profile scenario 1.



(b) Load profile scenario 2.



(c) Load profile scenario 3.

Figure 3.2: Active power load per radial. Based on [53].

3.3 Battery Case

One battery is used on connection with the case study network. The battery is connected to the first bus in radial 2, as presented in figure 3.3. The DSO can procure the necessary flexibility to ensure the power quality in the network. The battery is not connected to a specific end-user, however, the flexibility in the battery is accessible through a local flexibility market.

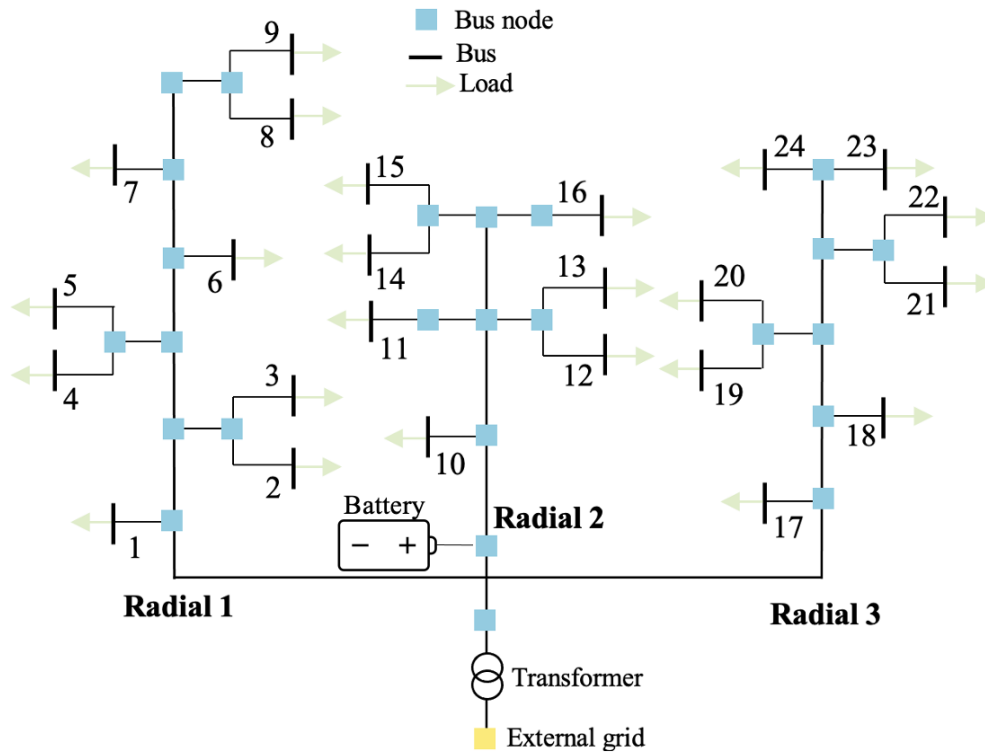


Figure 3.3: Placement of the battery in the case study.

Chapter 4

Methodology

This chapter presents the methods and modifications used to model, analyze and simulate the case study network. Further, the composition of the two-stage stochastic optimization model is presented. The objective of the model is to minimize the total cost for DSO while supplying the case study network with ample flexibility to maintain power quality and avoid under-voltage issues. The software used for modelling, as well as any model assumptions and limitations are presented. Lastly, the data and the data acquisition are presented.

4.1 Network Modeling and Simulation

This section presents software used to model and simulate the case study. It then presents an overview of the Test Feeder network the case study is based on. Thereafter, the process of modelling and simulating the case study network with any modifications, assumptions and approximations is presented.

4.1.1 Software: PandaPower

PandaPower is an open-source *Python* tool combining the system analysis tool, *PYPOWER*, and the data analysis library, *Pandas*. It is a power system analysis tool supporting element based power network modelling and several power system analysis methods, such as power flow analysis. *PandaPower* was developed by the University of Kassel and Fraunhofer Institute for Energy Economics and Energy System Technology (IEEE)[54][55].

PandaPower uses an element-based model (EBM) to model a network, and offers a library of elements based on electrical components, e.g. bus. An element is created by a set of input parameters, which might vary depending on the power system analysis method to be used. A standard library of pre-defined lines and transformers is also available [54][55]. *PandaPower* offers a time series simulation module to both analyze and simulate the network model. The module allows for a series of power flow simulations over a time period by the use of controllers, varying the the input data for a variable, e.g. active power. For each time step a controller simulation is initialized and a power flow analysis, using the Newton-Raphson method, is executed [54][56]. Figure 4.1 presents an overview over of the time series simulation module.

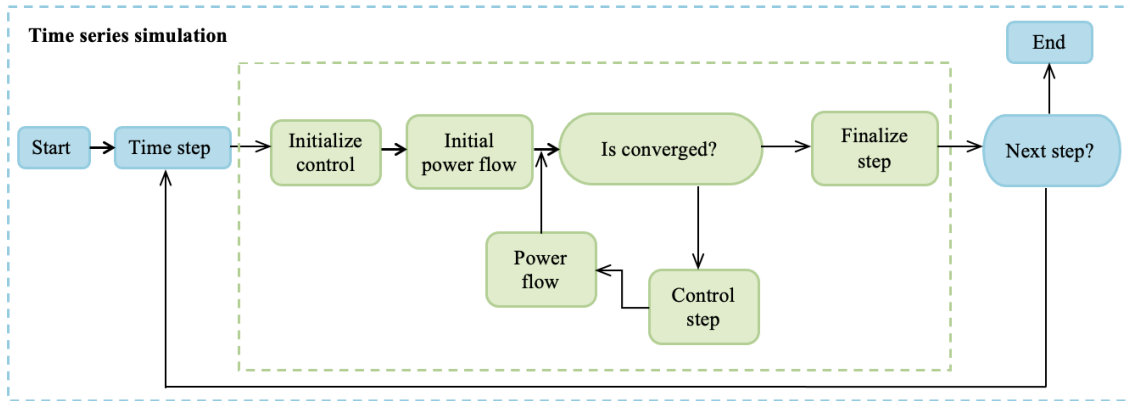


Figure 4.1: Time series simulation module overview. Based on [56].

4.1.2 Test Feeder Overview

The European Low Voltage Test Feeder network is a low voltage grid consisting of five components; buses, lines, loads, transformer and a voltage impedance source. The Test Feeder have 906 buses, where buses connected to a load have a rated voltage of 0.230 kV and the other buses have a rated voltage of 0.416 kV. The LV-side of the transformer is therefore connected to a 0.416 kV, the medium voltage (MV)-side is connected to the voltage source and the HV-side is connected to a bus with a rated voltage of 11 kV. The Test Feeder transformer is therefore a 11/0.416 kV three-winding transformer. There are 905 three-phase lines connecting the network together, and in total there are 55 loads distributed throughout the network. The Test Feeder grid is divided into three areas; Area A, Area B and Area C, as presented in figure 4.2 [52].

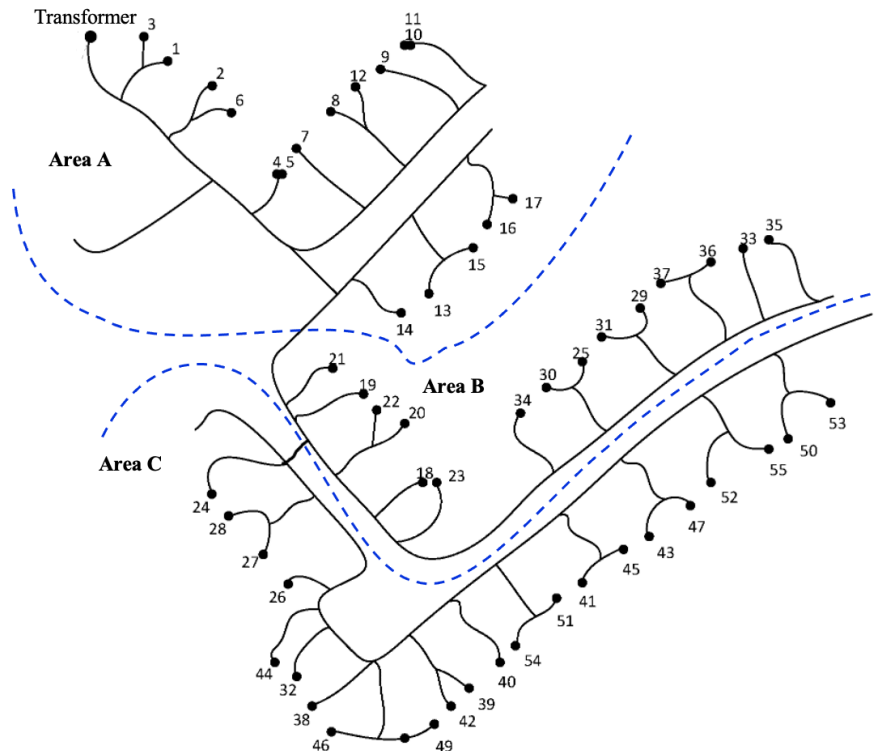


Figure 4.2: European Low Voltage Test Feeder network overview, where the loads are marked by numbers. Changes have been made from [57].

4.1.3 Network Modifications and Modeling

In most cases it is a goal to obtain a strong network, to avoid challenges such as under-voltage issues. However, in this case some modifications were made to weaken the grid and thereby obtaining under-voltage issues, as the results from the case study network were used for further analysis in the master thesis.

Only Area A in the Test Feeder network was used for further work in this master thesis. The other two areas were therefore removed. Some connections between buses and lines in Area A were changed to obtain a network with three radials. Further, two major assumptions were made for the modelling of the network in *PandaPower*, these are presented below. Smaller assumptions, approximations and changes made for specific network components are presented as the modelling of the components are described.

- **The same rated voltage at the LV-side**

There are two various rated voltages, 0.230 kV and 0.416 kV, used for the buses at the LV-side [52]. *PandaPower* does not support lines between buses of various rated voltages, the lines must therefore be modelled as transformers or the voltage must be set equal for all the buses at the LV-side [54]. It does not make sense to add transformers between buses and loads, therefore the voltages were set to 0.230 kV for all the buses on the LV-side.

- **Three-phase components were assumed to be single-phase**

All the three-phase components in the network were assumed to be single-phase and this was done by modelling them as single-phase elements in *PandaPower*. Excess available data meant for three-phase modelling was removed. Three-phase elements are supported by *PandaPower*, but the shift was made to single-phase to accommodate regular AC power flow.

Bus Elements

The bus element in *PandaPower* represents a node in the network, and all the other network elements must be connected to at least one bus, thereby binding the network together. A bus element is only defined by the rated voltage at the bus, as presented in 4.1 [54].

Table 4.1: Required input parameters for modelling bus elements in *PandaPower* [54].

Element	Input parameter	Unit
Bus	Rated voltage at bus	kV

Only the buses in Area A of the Test Feeder were kept, however, many of the buses acts as measuring nodes and were therefore not necessary. The only buses kept were buses connected to a load and buses used to split the grid in various directions. In addition, there are buses at the end of lines that were kept to be additional load buses. The network consist of one bus with a rated voltage of 11 kV connected to the HV-side of the transformer and 49 buses with a rated voltage of 0.230 kV buses at the LV-side.

Line Elements

In *PandaPower* line elements can be created by using line types offered in the standard type library or by input parameters. The required input parameters for single-phase lines are presented in table 4.2 [54]. The Test Feeder offers data for three-phase lines, however, this is also sufficient data for creating single-phase lines. The reduction of buses and the size of the network resulted in a reduced amount of lines, from 905 to 49. As unnecessary buses were removed the length of the lines were summed up, creating longer lines. The length of each line were multiplied by 15 to create even longer lines, but most importantly creating a weaker network. The Test Feeder uses various lines, which were kept. Information regarding line connections and line types are presented in appendix A.1 and appendix A.2, respectively.

Table 4.2: Required input parameters for modelling single-phase line elements in *PandaPower* [54].

Element	Input parameter	Unit
Line	To bus	-
	From bus	-
	Length	km
	Line resistance	Ω/km
	Line inductance	Ω/km
	Line capacitance	nF/km
	Max thermal current	kA

Load Elements

In *PandaPower* load elements represents electrical consumption and as load elements have a consumer viewpoint, loads are modelled by positive active- and reactive power. The required input parameters for load elements are presented in table 4.3 [54].

Table 4.3: Required input parameters for modelling load elements in *PandaPower* [54].

Element	Input parameter	Unit
Load	Active power	MW
	Reactive power	MVAr

As only Area A from the Test Feeder was used in the network, the number of loads were reduced from 55 to 17. However, additional buses at the end of lines were kept to create additional loads. The total amount of loads were therefore increased to 24. The data used to create the loads are from a modified version of a distribution grid at Steinkjer, Norway. The distribution grid at Steinkjer offers a wide range of load data, active- and reactive power, from 0.230 kV load buses over a time period from 25.01.2012 to 31.12.2012 with 15 minutes increments [53]. Various combinations of the loads were set together to obtain three load profile scenarios, as presented in section 3.2.

Transformer Element

PandaPower supports both two-winding and three-winding transformers [54]. The transformer used in the Test Feeder is a three-winding transformer, however, as the the voltage source at the MV-side of the transformer is removed, a two-winding transformer is sufficient. The transformer used is a 11/0.23 kV 0.8 MVA transformer, and all necessary input parameters, as presented in table 4.4, are available. All transformer parameters are presented in appendix A.3.

Table 4.4: Required input parameters for modelling a two-winding transformer element in *PandaPower* [54].

Element	Input parameters	Unit
Two-winding transformer	Low voltage bus	-
	High voltage bus	-
	Rated apparent power	MVA
	Rated high voltage	kV
	Rated low voltage	kV
	Short circuit voltage	%
	Real component of short circuit voltage	%
	Iron losses	kW
	Open loop losses	%
	Transformer phase shift angle	°

External Grid Element

The external grid element is a representation of the higher voltage grid the network is connected to, which in the Test Feeder is at the HV-side of the transformer. In *PandaPower* the external grid element is also used to create the slack bus for the network, which is needed for a power flow analysis. The required input parameters for modelling an external grid element are presented in table 4.5. As the external grid acts as a reference bus the voltage magnitude and angle were set to 1.0 pu and 0°, respectively [54].

Table 4.5: Required input parameters for modelling an external grid element in *PandaPower* [54].

Element	Input parameter	Unit
External grid	Connected bus	-
	Voltage set point	pu
	Angle set point	°

4.1.4 Network Simulation

The time series simulation module was used to simulate a power flow analysis of the case study network. The time period used for the simulation was from 30.01.12 to 08.02.12, as this is the period with the highest loads. Three assumptions were made for the simulation of the case study network, as presented below, and these are necessary assumptions for power flow analysis.

- The system is in steady-state condition
- The system is balance and symmetrical
- There are no faults or disturbances in the system

ConstControl

The time series simulation was done by the use of a controller, specifically a ConstControl. A ConstControl is created for a specific element, such as a load, which is specified by the use of the element index set by *PandaPower* as the element is created. In addition, the variable, e.g. active power, must be declared. The ConstControl reads the data from a data source based on a profile name, name of the column in the data source to be used, and then writes it back to the network. It was necessary to implement two controllers, to vary both the active- and reactive power in each time step according to the given load profiles [54].

Simulation Results

There are many various element results available from the time series simulation. The relevant results used for further work in this master thesis are presented in table 4.6.

Table 4.6: Relevant results available from *PandaPower* [54].

Element	Result
Bus	Voltage magnitude [pu]
Line	Current at bus [kA]

4.2 Optimization Model

This section presents the software used for modelling the two-stage stochastic optimization model. The optimization model is then presented with an explanation of model instances, such as sets and variables. The data used and the data acquisition are presented, as well as any assumptions and limitations.

4.2.1 Software: Pyomo and Gurobi Optimizer

Pyomo is an open-source optimization modeling language based on Python. *Pyomo* offers a diverse set of capabilities for modelling, analyzing and solving optimization models, and is therefore applicable for various problems, such as linear- and stochastic programming. The optimization problem is created by a mathematical representation of a system using the following concepts [58]:

- **Set:** Collection of elements used to define model instances such as variables
- **Variables:** Unknown or changing parts in the model
- **Parameters:** Known data supplied to the model to find the optimal solution for the variables
- **Constraints:** Mathematical relationships, such as equations or inequalities, connecting the parts of the model together
- **Objective:** Expression of variables to be minimized or maximized, the goal of the model

The solving of a model is done by the use of an external solver and *Pyomo* offers support to a variety of solvers, such as the *Gurobi Optimizer* [58]. The *Gurobi Optimizer* is a mathematical programming solver supporting a variety of modelling and programming languages, as well as various problem types [59].

4.2.2 Two-Stage Stochastic Optimization Model

The two-stage stochastic optimization model is based on the model presented in [46], however, changes and additions have been made. The goal of the two-stage stochastic optimization model is to procure enough flexibility, through a battery, to avoid violating set voltage limits. This is to be done considering the cost of booking and activating flexibility through two flexibility options, LongFlex and ShortFlex. The model also considers the degradation cost of the battery segments.

Sets and Indices

B/b	Set/index of batteries
J/j	Set/index of virtual battery segments
S/s	Set/index of scenarios
T/t	Set/index of time steps

Parameters

ΔT	Conversion factor kW to kWh
η_b^{ch}	Battery b charging efficiency [%]
η_b^{dis}	Battery b charging efficiency [%]
ρ_s	Probability of scenario s [%]
$C_t^{booking}$	Cost of booking LongFlex [NOK/kWh]
C_t^{long}	Cost of activating LongFlex [NOK/kWh]
C_t^{short}	Cost of activating ShortFlex [NOK/kWh]
C_{bj}^{deg}	Cost of segment j in battery b [NOK/kWh]

E_b^{cap}	Energy capacity of battery b [kWh]
E_{bj}^{cap}	Energy capacity of segment j in battery b [kWh]
F_{bst}^{load}	Flexibility demand per battery b [kW]
Q_b^{ch}	Maximum battery b charging power [kW]
Q_b^{dis}	Maximum battery b discharging power [kW]
X_{bst}^{imp}	Available charging power per battery b [kW]

Variables

δ_{bt}	Battery b binary variable
$\hat{\delta}_{bst}$	Second stage battery b binary variable
$a_{st}^{long\uparrow}$	Activated upward flexibility through LongFlex [kW]
$a_{st}^{short\uparrow}$	Activated upward flexibility through ShortFlex [kW]
e_{bt}	Battery b state of charge [kWh]
\hat{e}_{bst}	Second stage battery b state of charge [kWh]
\hat{e}_{bstj}^{seg}	Second stage battery b segment j state of charge [kWh]
q_{bt}^{ch}	Battery b charging power [kW]
\hat{q}_{bst}^{ch}	Second stage battery b charging power [kW]
$\hat{q}_{bstj}^{ch,seg}$	Second stage battery b segment j charging power [kW]
q_{bt}^{dis}	Battery b discharging power [kW]
\hat{q}_{bst}^{dis}	Second stage battery b discharging power [kW]
$\hat{q}_{bstj}^{dis,seg}$	Second stage battery b segment j discharging power [kW]
$r_t^{long\uparrow}$	Booked upward capacity through LongFlex [kW]

Objective Function

The main objective function for the optimization model is presented in equation 4.1. The first term is related to the first stage and the total cost of booking LongFlex by multiplying the booked LongFlex, $r_t^{long\uparrow}$, with the cost of booking LongFlex, $C_t^{booking}$. The second and third term are the second stage cost of activating flexibility, through LongFlex, $a_{st}^{long\uparrow} \cdot C_t^{long}$, and ShortFlex, $a_{st}^{short\uparrow} \cdot C_t^{short}$, multiplied with the probability of each scenario, ρ_s .

$$\begin{aligned}
 \min \quad & \sum_t \Delta T \cdot r_t^{long\uparrow} \cdot C_t^{booking} + \sum_s \rho_s \sum_t \Delta T \cdot a_{st}^{long\uparrow} \cdot C_t^{long} \\
 & + \sum_s \rho_s \sum_t \Delta T \cdot a_{st}^{short\uparrow} \cdot C_t^{short} + \sum_b \sum_s \rho_s \sum_t \sum_j \Delta T \cdot \hat{q}_{bstj}^{dis,seg} \cdot C_{bj}^{deg} \quad (4.1)
 \end{aligned}$$

The fourth term is the total cost of battery degradation. This is obtained by multiplying the second stage segmented battery discharge, $\hat{q}_{bstj}^{dis,seg}$ with the cost of battery degradation, C_{bj}^{deg} , and the probability of each scenario, ρ_s . ΔT is used in every term to convert kW to kWh, as the costs are given by NOK/kWh and the power related variables are in kW.

Constraints

The flexibility demand, F_{bst}^{load} , is the flexibility to be procured by each battery to uphold the set voltage limit. To ensure that all the flexibility demand is covered, the sum of the activated upward capacity from LongFlex and ShortFlex, $a_{st}^{long\uparrow} + a_{st}^{short\uparrow}$, must be equal to or greater than the flexibility demand, as stated in equation 4.2.

$$a_{st}^{long\uparrow} + a_{st}^{short\uparrow} \geq \sum_b F_{bst}^{load} \quad \forall st \quad (4.2)$$

Equation 4.3 states the energy balance in the network and ensures available power for battery charging in time steps without flexibility demand. The available charging power, X_{bst}^{imp} , and the second stage discharging, \hat{q}_{bst}^{dis} must be equal to or greater than the flexibility demand, F_{bst}^{load} , and second stage charging, \hat{q}_{bst}^{ch} .

$$X_{bst}^{imp} + \hat{q}_{bst}^{dis} \geq F_{bst}^{load} + \hat{q}_{bst}^{ch} \quad \forall bst \quad (4.3)$$

Equation 4.4a states that the deviation from the baseline, $\sum_b (\hat{q}_{bst}^{dis} - q_{bt}^{dis})$, for each scenario cannot exceed the sum of the booked upward capacity through LongFlex, $r_t^{long\uparrow}$. The same goes for the activated upward flexibility through LongFlex, $a_{st}^{long\uparrow}$, as presented in equation 4.4b.

$$r_t^{long\uparrow} \geq \sum_b (\hat{q}_{bst}^{dis} - q_{bt}^{dis}) \quad \forall st \quad (4.4a)$$

$$r_t^{long\uparrow} \geq a_{st}^{long\uparrow} \quad \forall st \quad (4.4b)$$

Equation 4.5a, 4.5b and 4.5c are first stage battery constraints. Equation 4.5a is the maximum charging constraint, ensuring that the battery charging power, q_{bt}^{ch} , has to be less than or equal to the maximum battery charging power, Q_b^{ch} , if the battery is not in use, which is defined by the battery binary variable $\delta_{bt} = 1$. The maximum discharging constraint is given by equation 4.5b, where the battery discharging power, q_{bt}^{dis} , has to be less than or equal to the maximum battery discharging power parameter, Q_b^{dis} , if the battery is in use, $\delta_{bt} = 0$. The battery SOC e_{bt} limit is set in equation 4.5c by the energy capacity of the battery, E_b^{cap} .

$$q_{bt}^{ch} \leq Q_b^{ch} \cdot \delta_{bt} \quad \forall bt \quad (4.5a)$$

$$q_{bt}^{dis} \leq Q_b^{dis} \cdot (1 - \delta_{bt}) \quad \forall bt \quad (4.5b)$$

$$0 \leq e_{bt} \leq E_b^{cap} \quad \forall bt \quad (4.5c)$$

Equation 4.6a, 4.6b and 4.6c are second stage battery constraints, stating the same as the first stage battery constraints. The second stage battery constraints uses the second stage charging power, \hat{q}_{bst}^{ch} , second stage discharging power, \hat{q}_{bst}^{dis} , the second stage binary variable, $\hat{\delta}_{bst}$, and the second stage battery SOC, \hat{e}_{bst} .

$$\hat{q}_{bst}^{ch} \leq Q_b^{ch} \cdot \hat{\delta}_{bst} \quad \forall bst \quad (4.6a)$$

$$\hat{q}_{bst}^{dis} \leq Q_b^{dis} \cdot (1 - \hat{\delta}_{bst}) \quad \forall bst \quad (4.6b)$$

$$0 \leq \hat{e}_{bst} \leq E_b^{cap} \quad \forall bst \quad (4.6c)$$

The link between the second stage segmented battery variables and the second stage non-segmented variables are given in equation 4.7a, 4.7b and 4.7c. In equation 4.7a the sum of the second stage battery segments SOC, \hat{e}_{bstj}^{seg} , is set to be equal to the second stage battery SOC, \hat{e}_{bst} . The sum of the second stage battery segments charging power, $\hat{q}_{bstj}^{ch,seg}$, is set equal to the second stage charging power, \hat{q}_{bst}^{ch} , as presented in equation 4.7b. The same is stated for the second stage battery segments discharging power, $\hat{q}_{bstj}^{dis,seg}$, and second stage discharging power, \hat{q}_{bst}^{dis} , in equation 4.7c.

$$\sum_j \hat{e}_{bstj}^{seg} = \hat{e}_{bst} \quad \forall bst \quad (4.7a)$$

$$\sum_j \hat{q}_{bstj}^{ch,seg} = \hat{q}_{bst}^{ch} \quad \forall bst \quad (4.7b)$$

$$\sum_j \hat{q}_{bstj}^{dis,seg} = \hat{q}_{bst}^{dis} \quad \forall bst \quad (4.7c)$$

Equation 4.8a states that the second stage battery SOC per segment, \hat{e}_{bstj}^{seg} , is limited by the energy capacity per battery segment, E_{bj}^{cap} . The sum of the SOC per battery segment, $\sum_j \hat{e}_{bstj}^{seg}$, is limited by the battery capacity, E_b^{cap} , as presented in equation 4.8b.

$$0 \leq \hat{e}_{bstj}^{seg} \leq E_{bj}^{cap} \quad \forall bstj \quad (4.8a)$$

$$0 \leq \sum_j \hat{e}_{bstj}^{seg} \leq E_b^{cap} \quad \forall bst \quad (4.8b)$$

Equation 4.9a states the evolution of the battery SOC for the state $t = t + 1$, $e_{b(t+1)}$, is then equal to e_{bt} plus the charging power, q_{bt}^{ch} , times the charging efficiency, η_b^{ch} , minus the discharging power, q_{bt}^{dis} , divided by the discharging efficiency, η_b^{dis} . Equation 4.9b states the same for the second stage segmented battery SOC, $\hat{e}_{bs(t+1)j}$. ΔT is used to convert kW to kWh.

$$e_{b(t+1)} = e_{bt} + \Delta T \left(\eta_b^{ch} \cdot \hat{q}_{bt}^{ch} - \frac{\hat{q}_{bt}^{dis}}{\eta_b^{dis}} \right) \quad \forall bt \quad (4.9a)$$

$$\hat{e}_{bs(t+1)j} = \hat{e}_{bstj} + \Delta T \left(\eta_b^{ch} \cdot \hat{q}_{bstj}^{ch} - \frac{\hat{q}_{bstj}^{dis}}{\eta_b^{dis}} \right) \quad \forall bstj \quad (4.9b)$$

4.2.3 Model Limitations

There are several limitations of the model. Firstly, the battery “injects” active power into the network model to cover the flexibility demand, however, the effects of this on the network is not accounted for. The optimization model does not account for “injected” active power causing any overloading of lines or voltage issues at buses. Further, power is made available for charging the battery and the effect of this power on the network is not accounted for considering overloading and voltage issues. As flexibility is used to cover the flexibility demand, further effects of cover flexibility demand are not accounted for. Meaning, the model does not investigate how 1 kW from the battery might effect the flexibility demand or other part of the network before using more of the flexibility available in the battery.

4.2.4 Data

The data used in the optimization model for sets and parameters are presented below with an explanation of acquisition of the data.

Declaration of Sets

The parameters, variables and constraints are defined by the use of four sets. The sets and their respective data are presented in table 4.7. The number of batteries in set B is one, based the battery case, presented in section 3.3. The number of virtual battery segments in set J are set to 10. The three load profile scenarios presented in section 3.2 are basis for set S . Set T are the number of time steps from 30.01.12-08.02.12, as this is the time period with flexibility demand.

Table 4.7: *The sets in the optimization model and their respective data.*

Set	Description	Data
B	Batteries	1
J	Virtual battery segments	10
S	Scenarios	3
T	Time steps	864

Procuring the Flexibility Demand

The flexibility demand for each of the three load profile scenarios implemented in the optimization model was calculated using the results from the network model. The results acquired from the network model were the voltage magnitude and current at each bus. A function was created using *Python* to calculate the various flexibility demands. The function finds out the buses with load, takes the voltages magnitude results for these buses and find the load buses with voltage below a set limit.

The function then calculates the amount of voltage below that limit for each load bus and multiplies it with the current at that specific bus. The results from the function are then the flexibility demand to be procured for each load bus to not exceed the set voltage limit. Two various voltage limits were set, as presented below, creating two voltage limit cases. Each voltage limit case has three various flexibility demand scenarios based on the three load profile scenarios.

- **Under-voltage limit:** The under-voltage limit was set to 0.9 pu as any violations of this limit results in statutory voltage limit violations and thereby creates under-voltage issues in the case study network.
- **Power quality limit:** The power quality limit was set to 0.95 pu and it is set to maintain the power quality in the network. It also ensures that there are no violations of statutory voltage limits and thereby no under-voltage issues.

There is only one battery connected to the network in the case study, meaning that one battery must cover the whole flexibility demand. The flexibility demand was therefore summed up for each scenario, leading to a flexibility demand per scenario, per time step for each of the two voltage cases.

Probability Scenarios

The three load profile scenarios lead to three various flexibility demand scenarios for each voltage limit case. There was no basis for assuming various probabilities for each load profile scenario as there were no data to support this. Therefore it was assumed that the probability of the three various flexibility demand scenarios for each voltage limit case were equal, as presented in table 4.8.

Table 4.8: The probability of each load profile/flexibility demand scenario.

Scenario	Probability
1	0.333
2	0.333
3	0.333

Cost of Flexibility

Two profiles for the cost of flexibility were created for use in the optimization model. There is no basis for setting the cost of flexibility due to limited market data. These costs are therefore not representative for the actual cost of flexibility, but rather to test two various cost situations.

- Cost of flexibility profile 1:** In the first profile the total cost of booking and activating LongFlex is equal to the cost of activating ShortFlex per time step. Thereby making it up to the optimization model to find the minimized cost combination of ShortFlex and LongFlex with equal costs. The cost used are presented in table 4.9.

Table 4.9: Cost of flexibility profile 1.

Service	Cost
ShortFlex activation	1.5 NOK/kWh
LongFlex booking	0.5 NOK/kWh
LongFlex activation	1.0 NOK/kWh

- Cost of flexibility profile 2:** The costs in the second profile were based on market data from *Nordpool* in the period 28.08.21-02.10.21. Market data is given per hour, however, in the model the cost per hour was set as the cost per 15 minutes. Area 1 in Denmark was used for the cost of activating ShortFlex, while area Oslo was used for the cost of activating LongFlex. The cost for booking LongFlex were set to 0.3 NOK/kWh. The most important factors for using this data were that these are market prices for electricity and the two cost profiles vary around each other, as presented in figure 4.3.

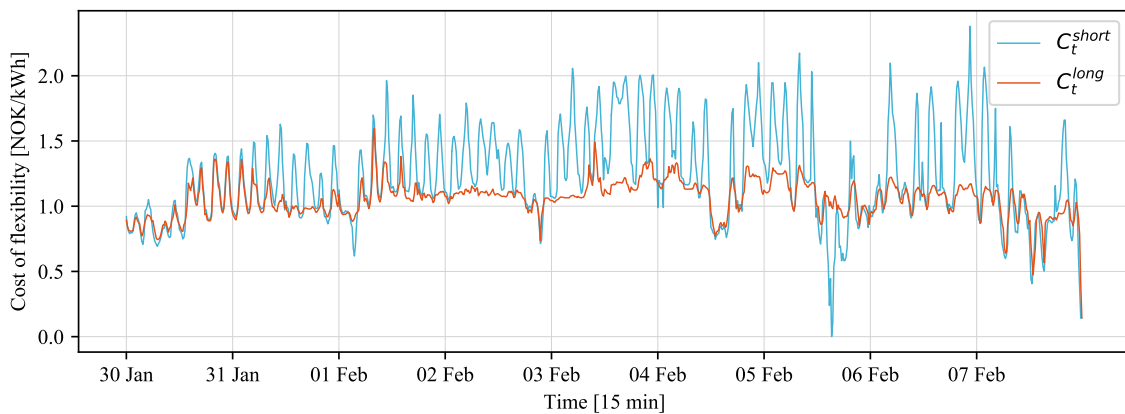


Figure 4.3: Cost of flexibility in cost profile 2. Based on data from [60].

Batteries

The battery specifications for the battery used in the model is based on technical data for the *sonnenBatterie hybrid 9.53*. The *hybrid 9.53* is a high-tech battery storage system offering a battery capacity between 2.5-15 kWh, using Lithium Iron Phosphate cell technology. Additionally, the *hybrid 9.53* has a DoD of 90 % and a cycle life of 10 000 cycles [61][62]. The specifications for the battery used in the optimization model are presented in 3.3.

Table 4.10: Battery specifications for the case study battery. Based on data from [61] and [62].

Cost	Capacity	Maximum charging	Maximum discharging	Charging efficiency	Discharging efficiency
63131.38 NOK	15 kWh	3.3 kW	3.3 kW	95 %	95 %

Cost of Battery Degradation

The cost of battery degradation was set using the method from reference [43] presented in section 2.3.4. Table 4.11 presents the parameters used to calculate the cost of degradation per segment in NOK/kWh.

Table 4.11: Parameters used for battery degradation. Based on data from [61] and [62].

Parameters	
Replacement cost	63131 NOK
Discharge efficiency	95 %
Energy capacity	15 kWh
Segments	10
Life loss per full cycle	0.0001

The degradation cost per battery segment is presented in figure 4.4

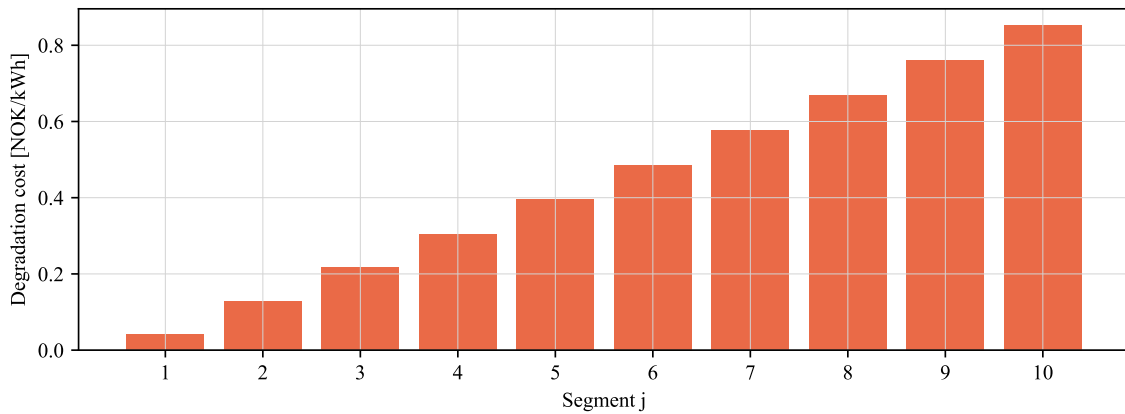


Figure 4.4: Degradation cost per battery segment. Based on method from [43].

Imported Charging Power

The imported power in the model acts as offered power to charge the battery in time steps where there is no flexibility demand. If charging power is offered in a time step, it is set to 1 kW per battery used in the model. It is therefore always available power for the battery to charge.

Chapter 5

Results and Discussion

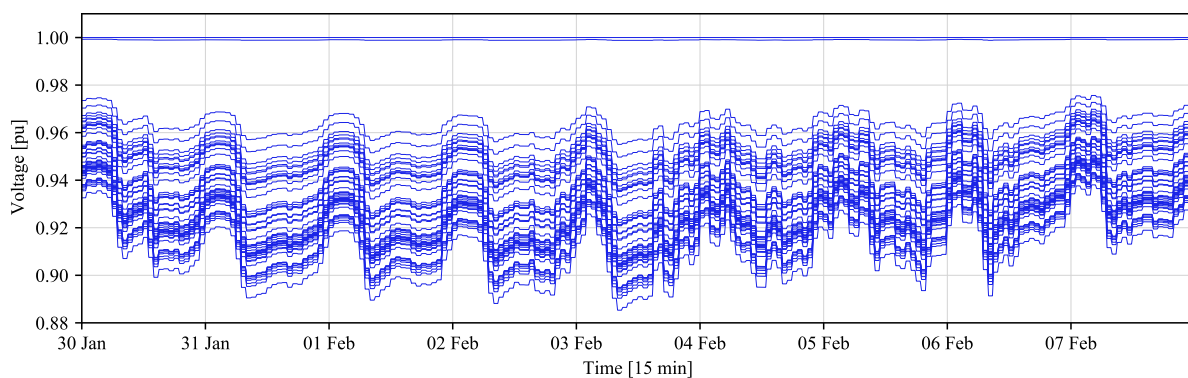
This chapter presents the results from the simulation of the network model using the various load profile scenarios. The demand for flexibility in the case study network is presented considering two voltage limits. Further, the results from the two-stage optimization model using the various flexibility demands and two cost of flexibility scenarios are presented. This chapter also presents a discussion of the results as they are presented.

5.1 Network Model

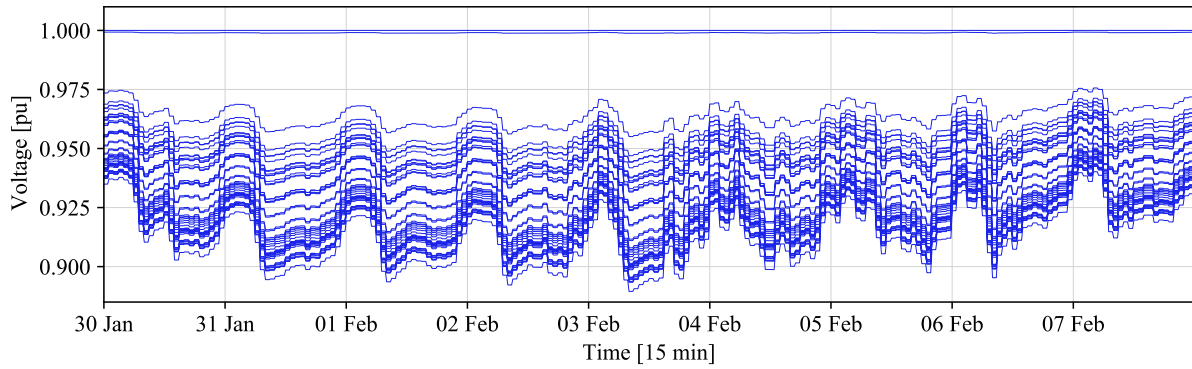
This section presents the results obtained from the power flow time series simulation of the network model. This includes results such voltage magnitude profiles compared to the two voltage limits; under-voltage and power quality. Further, it presents the flexibility obtained from the network results using the various load profile scenarios and the voltage limits.

5.1.1 Voltage Magnitude

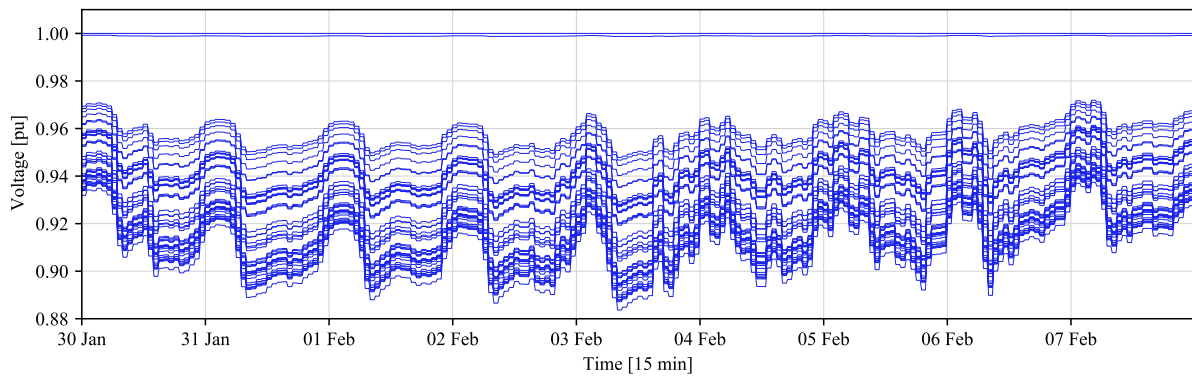
The results from the network model were obtained using three various load profiles, as presented in section 3.2, and the voltage magnitude profile for each bus, in each load profile scenario were obtained, as presented in figure 5.1. Figure 5.1a presents the voltage magnitude results from load profile 1, and the voltage magnitude ranges from 1 pu to 0.885 pu, resulting in under-voltage issues. These under-voltage issues vary between long and very long duration.



(a) Load profile scenario 1.



(b) Load profile scenario 2.



(c) Load profile scenario 3.

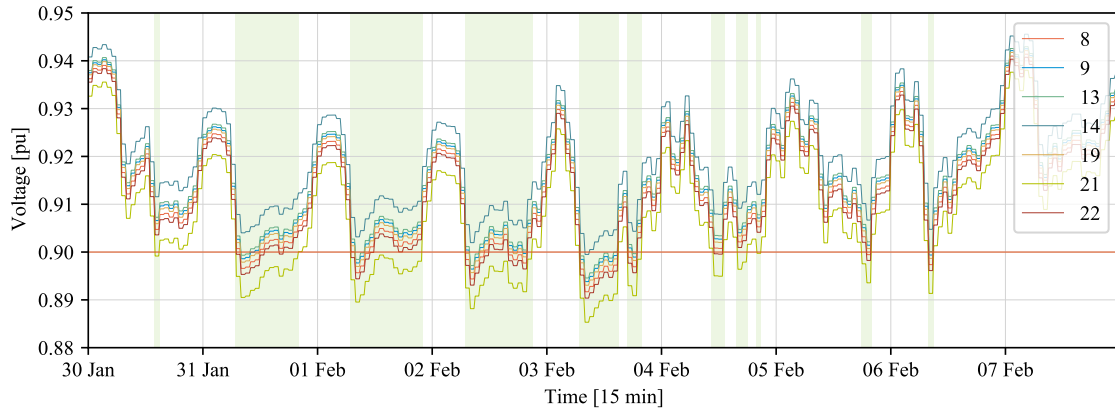
Figure 5.1: Voltage magnitude profiles for all buses for each load profile scenario.

The voltage magnitude results from using load profile scenario 2 in the network model is presented in figure 5.1b. The use of load profile scenario 2 also results in long and very long duration under-voltage issues. The voltage magnitude varies between 1 pu to 0.8895 pu, which is slightly higher than the lowest voltage magnitude from the use of load profile scenario 1. Figure 5.1c presents the voltage magnitudes obtained from using load profile scenario 3. The voltage magnitude is between 1 pu and 0.8836 pu.

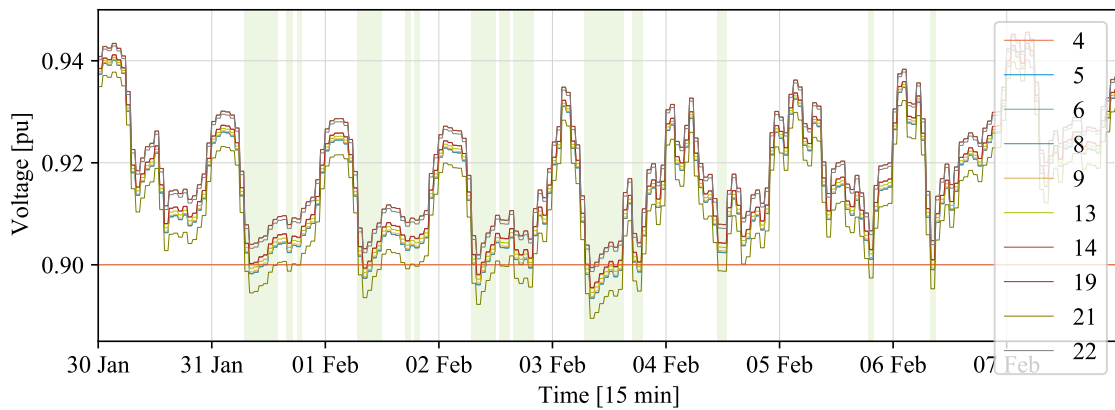
The use of all the various load profile scenarios in the network model results under-voltage issues. This is expected as some of the modifications made while creating the case study network were done to create a weakened network and thereby creating under-voltage issues. The under-voltage issues across the three load profile scenarios are of varying degree, where load profile scenario 3 leads to the lowest magnitude of 0.8836, and of varying duration.

5.1.2 Under-Voltage Issues

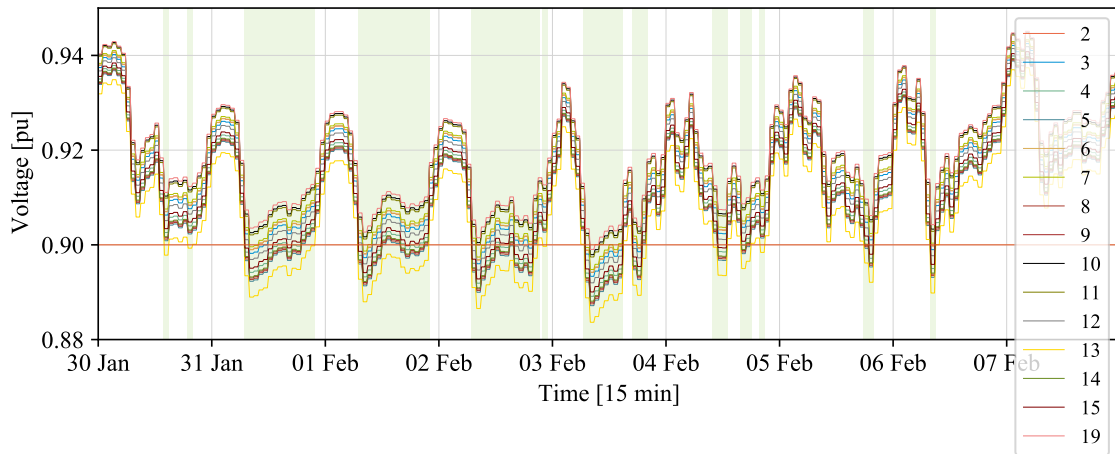
Figure 5.2 presents the voltage magnitude of the load buses in each load profile scenario violating the under-voltage limit of 0.9 pu, and all time steps with one or more violation are marked. The results from the use of load profile scenario 1 are presented in figure 5.2a. Load profile scenario 1 creates 11 time periods with a varying degree of time and violations, which are divided between the load buses from all of the three radial in the case study network. There are 7 load buses with violations; load bus 8 and 9 at radial 1, load bus 13 and 14 at radial 2 and load bus 19, 21 and 22 at radial 3.



(a) Load profile scenario 1.



(b) Load profile scenario 2.



(c) Load profile scenario 3.

Figure 5.2: Voltage magnitude profiles for load buses violating the under-voltage limit of 0.9 pu

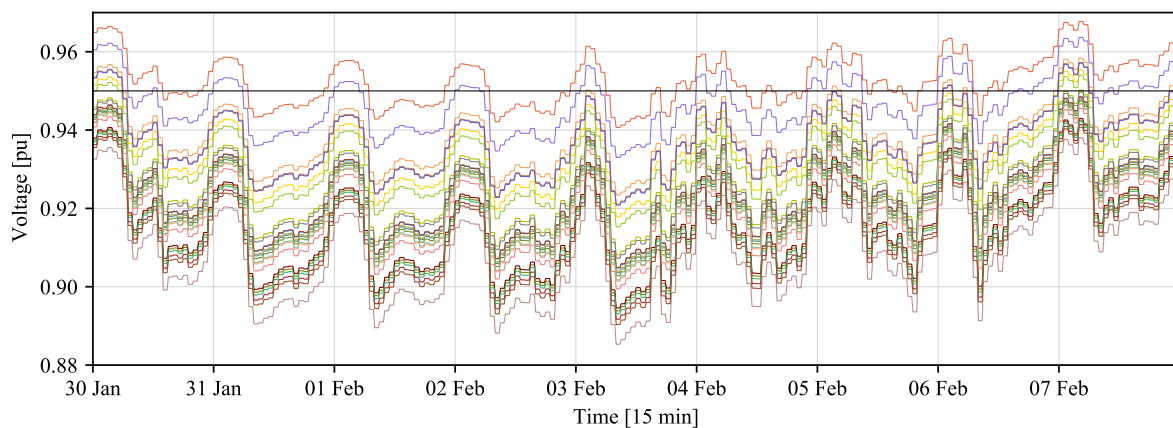
Figure 5.2b presents the load buses violating the under-voltage limit with the use of load profile scenario 2. By comparing this figure with figure 5.2a it can be observed that load profile scenario 2 results in 3 more time periods with violations. However, these are shorter time periods compared to time periods from the use of load profile scenario 1. Further, load profile scenario 2 leads to an increased amount of load buses with violations, in total 10. The additional load buses with violations are load bus 4, 5 and 6, leading to greater under-voltage issues at radial 1.

The results from the use of load profile scenario 3 are presented in figure 5.2c. The use of load profile scenario 3 results in violations at all the load buses at radial 1, except load bus 1, and at all the load buses at radial 2, except load bus 16. Thereby increasing the violations at radial 1 and 2, while decreasing the violations at radial 3, where there only are violations from load bus 19. Even though load profile scenario 3 leads to violations at 15 buses, the amount of time periods with violations are 13, compared to 11 and 14 from load profile scenario 1 and 2, respectively.

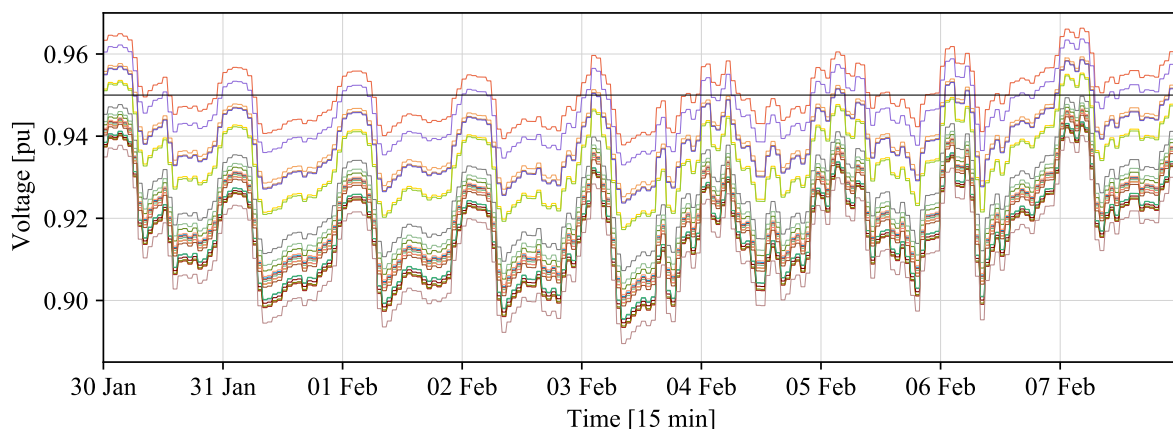
Compared with each other, load profile scenario 3 leads to the greatest amount of load buses with violations. However, the degree of violations vary from load bus to load bus, and from load profile scenario to load profile scenario. The same can be said for the duration of the time periods with violations.

5.1.3 Power Quality Issues

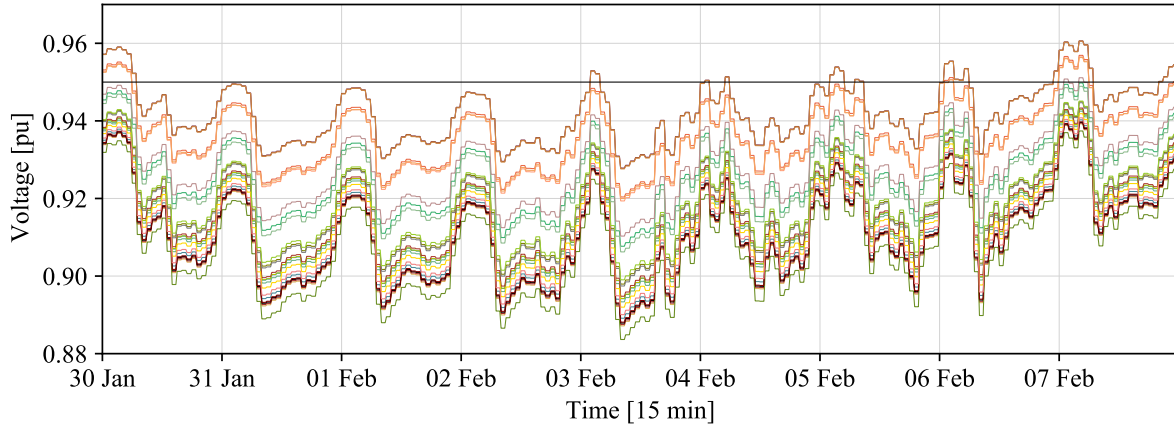
Figure presents the voltage magnitude of the load buses violating the power quality voltage limit of 0.95, for all the load profile scenarios. The results are presented in figure 5.3a for load profile scenario 1, figure 5.3b for load profile scenario 2 and figure 5.3c for load profile scenario 3.



(a) Load profile scenario 1.



(b) Load profile scenario 2.



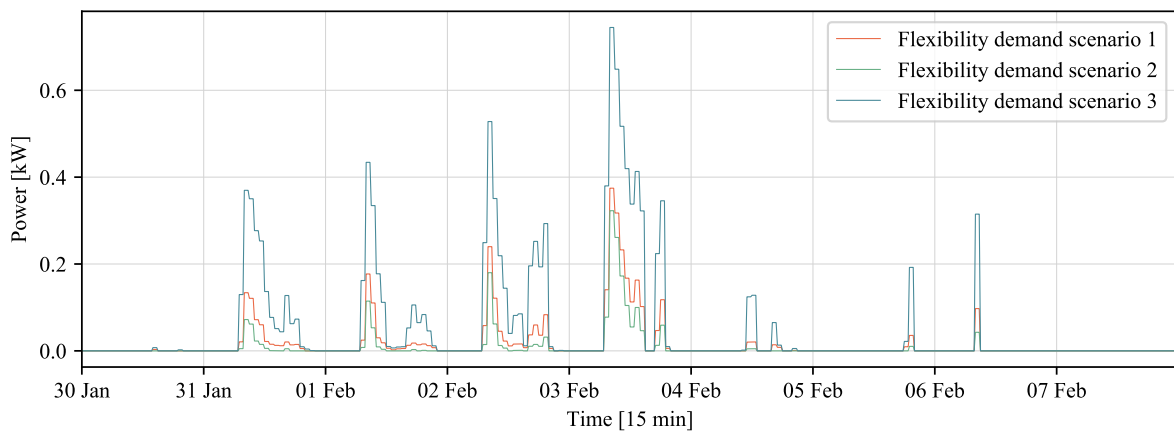
(c) Load profile scenario 3.

Figure 5.3: Voltage magnitude profiles for load buses violating the power-quality limit of 0.95 pu

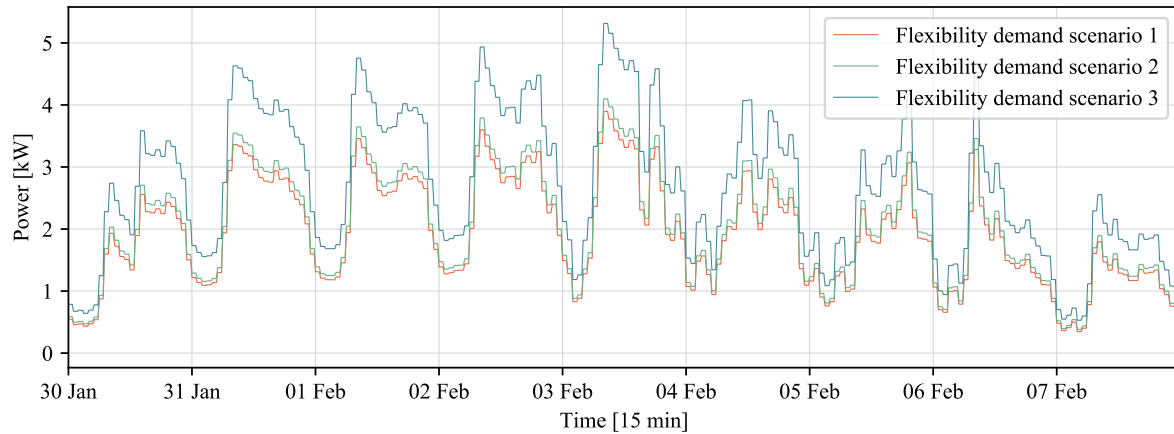
By comparing these figures it can be observed that all of the three load profile scenarios results in one or more violations at all of the load buses. The power quality voltage limit leads to constant violations during the given time frame, and most of the load buses are in a constant violation of the limit. This expected from the results of the under-voltage limit in figure 5.2, as the only change from those results is an increased voltage limit.

5.1.4 Flexibility Demand

Figure 5.4 presents the flexibility demands from the use of all the load profile scenarios considering the two voltage limits; under-voltage and power quality. The flexibility demands from the load profile scenarios when considering the under-voltage limit at 0.9 are presented in figure 5.4a. From the figure it can be observed that load profile scenario 3 leads to the greatest flexibility demand. This was expected as the voltage magnitude for load buses creating violations of the under-voltage limit, was the greatest compared the same result from using load profile scenario 1 and 2, as presented in figure 5.2. The flexibility demands from load profile scenario 1 and 2 are quite similar, however, the flexibility demand from load profile scenario 1 is slightly higher.



(a) Under-voltage limit.



(b) Power quality voltage limit.

Figure 5.4: Flexibility demands for each load profile scenario as result of the two voltage limits, under-voltage and power quality.

Figure 5.4b presents the flexibility demands from setting the voltage limit at 0.95. This results in a constant flexibility demand from the use of each of the three load profile scenarios. The three load profile scenarios creates three various flexibility demand scenarios for each of the two voltage limits. The load profile scenarios are therefore referred to as flexibility demand scenarios for the rest of this chapter, dependent on which load profile scenario the flexibility demand comes from.

The method used for procuring the flexibility demand is quite simple, as it is done by multiplying the current at the bus with the voltage magnitude below the set voltage limit. This method does not account for how the flexibility demand might change as a result of flexibility “injected” into the network from the battery in previous time steps.

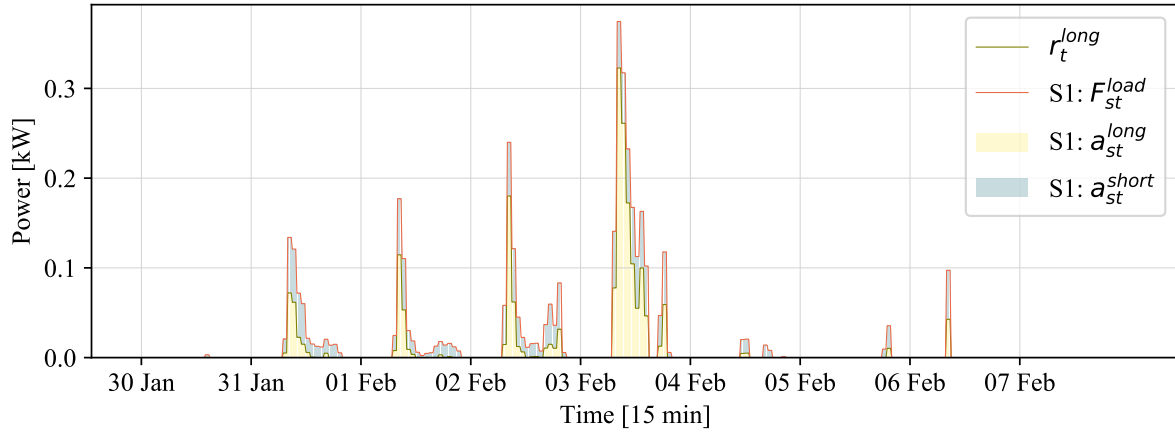
5.2 Optimization Model

This section presents the results from the two-stage stochastic optimization model using the flexibility demands acquired from the results of the network model. Firstly, the results from using the under-voltage limit are presented and then the results from power-quality voltage limit.

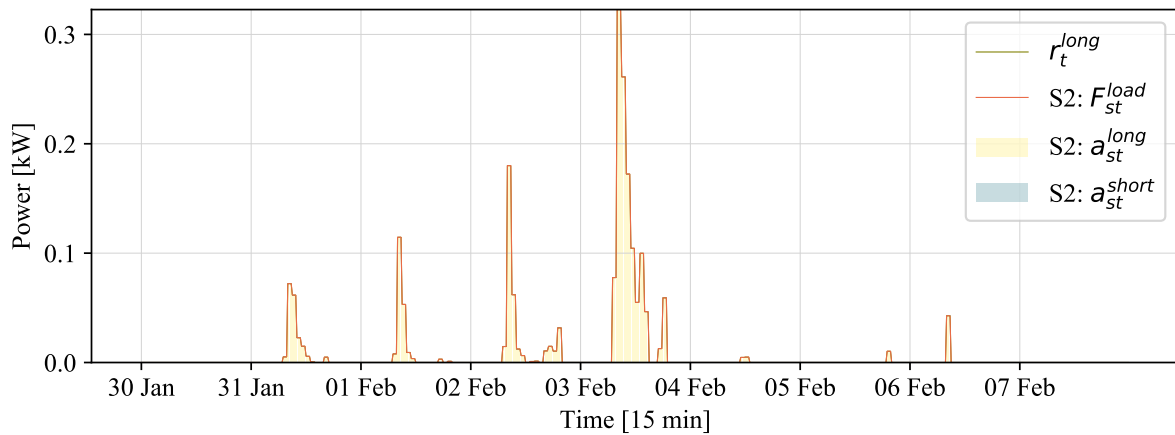
5.2.1 Under-Voltage Issues

Activation and Booking

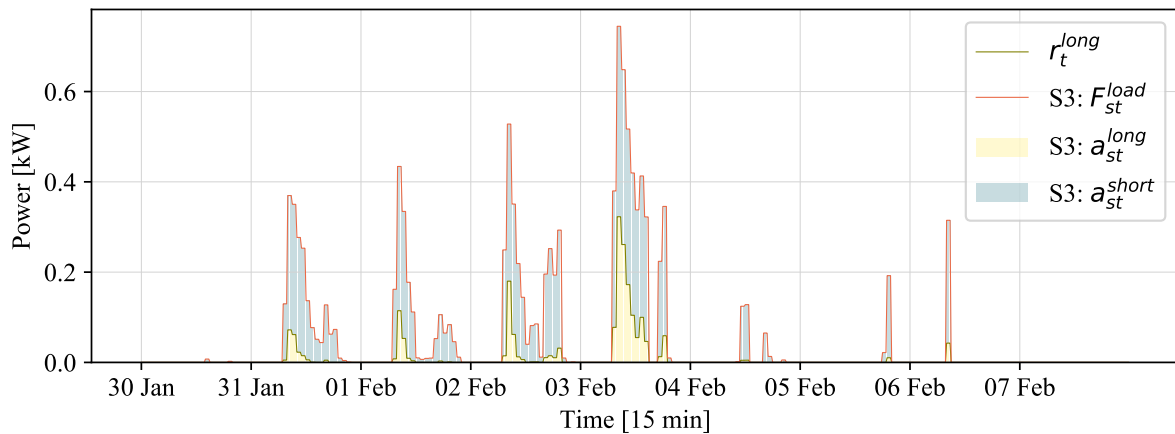
The first stage decision of booking LongFlex and the second stage decisions for activating LongFlex and ShortFlex for each flexibility demand scenario using cost of flexibility profile 1 are presented in 5.5. The results are presented for flexibility demand scenario 1 in figure 5.5a, for flexibility demand scenario 2 in figure 5.5b and flexibility demand scenario 3 in 5.5c. From figure 5.5b it can be observed that the whole flexibility demand in scenario 2 is covered by LongFlex. However, in flexibility demand scenario 1 and 2, ShortFlex is also activated to cover the demand.



(a) Flexibility demand scenario 1.



(b) Flexibility demand scenario 2.

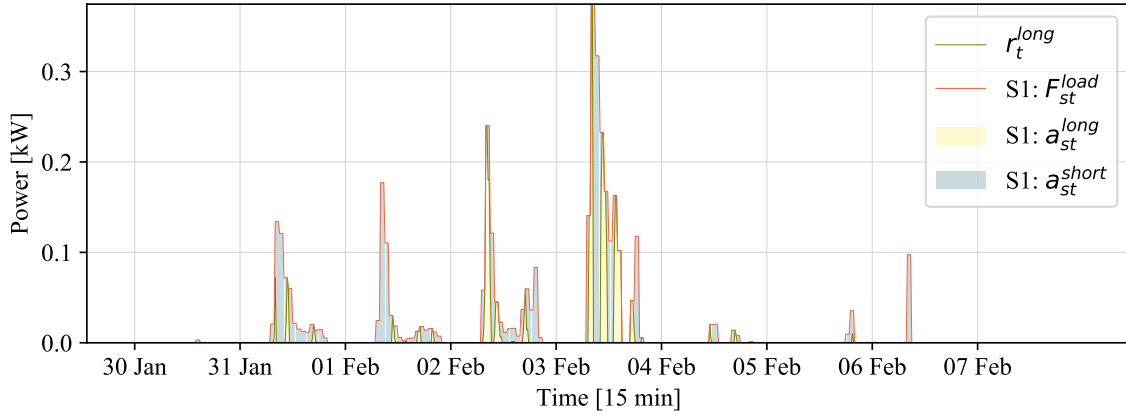


(c) Flexibility demand scenario 3.

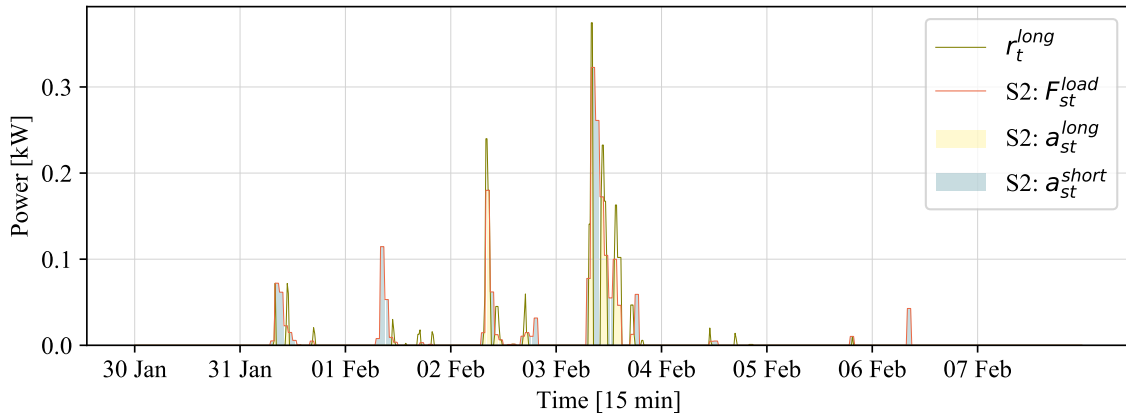
Figure 5.5: Booking and activation of LongFlex and activation of ShortFlex using cost of flexibility profile 1.

It can also be observed from figure 5.5a and figure 5.5c that all the LongFlex booked in stage 1 is activated in stage 2. Cost profile 1 was used, and in time steps with flexibility demand across each scenario, it is cheaper to book and activate LongFlex. This is because the cost of booking LongFlex is not a scenario dependent variable in the optimization model. The booked LongFlex is therefore usable in all three scenarios, but only paid for once, making the total cost lower.

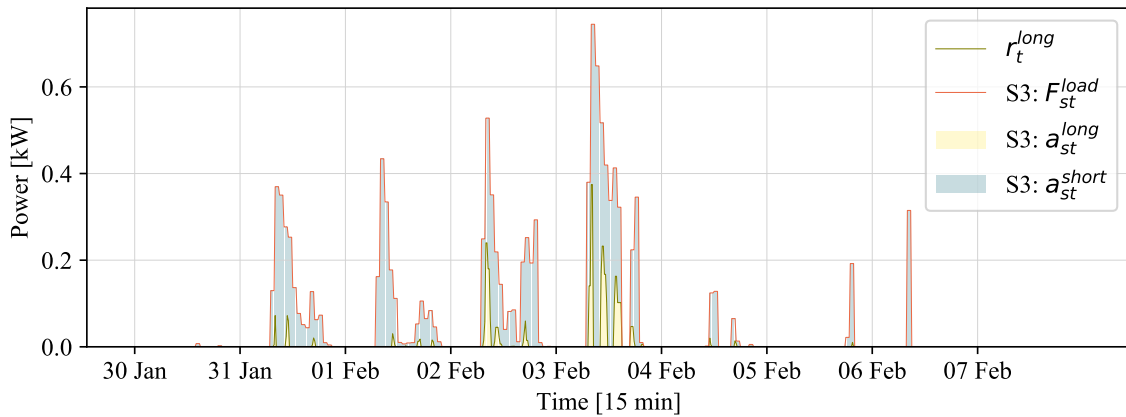
The booking and activation of LongFlex and the activation of ShortFlex for each flexibility demand scenario using cost of flexibility profile 2 are presented in figure 5.6. These results are presented in figure 5.6a for flexibility demand scenario 1, figure 5.6b for flexibility demand scenario 2 and figure 5.6c for flexibility demand scenario 3. It can be observed from figure 5.6 that both ShortFlex and LongFlex are activated for all three scenarios. The varying use of ShortFlex and LongFlex is a result of the varying cost of ShortFlex and LongFlex. In some time steps it is cheaper to activated ShortFlex for each flexibility demand scenario, rather than booking and activating LongFlex, and the other way around.



(a) Flexibility demand scenario 1.



(b) Flexibility demand scenario 2.



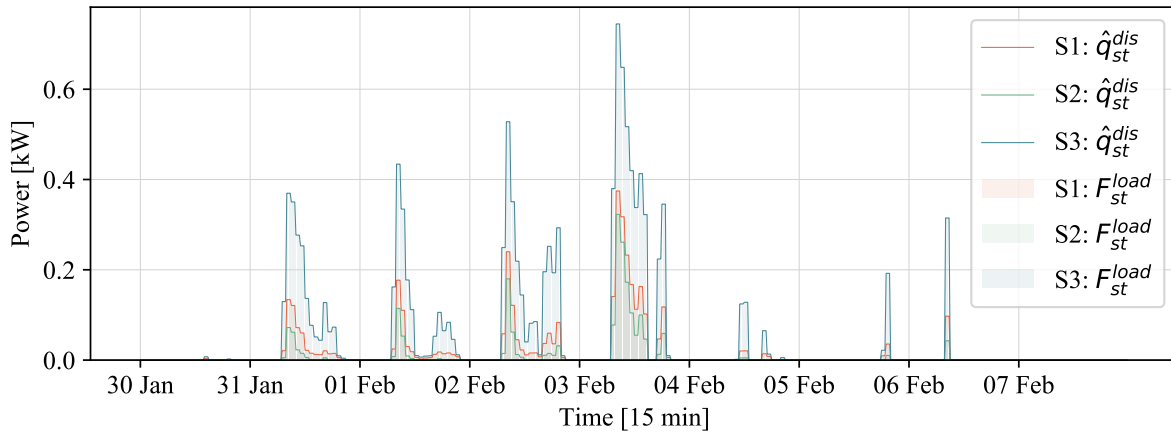
(c) Flexibility demand scenario 3.

Figure 5.6: Booking and activation of LongFlex and activation of ShortFlex using cost of flexibility profile 2.

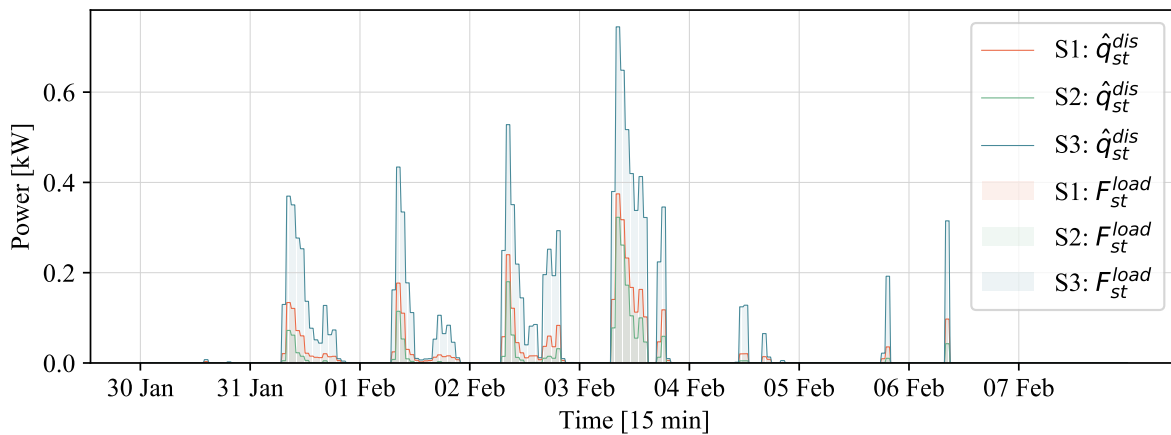
Further, the optimization model states that the amount of booked flexibility must be greater than or equal to the activated LongFlex. The booked LongFlex is never below the activated LongFlex, however, in figure 5.6b it can be observed that the booked LongFlex exceeds the amount of activated LongFlex. This is a result of the amount of booked LongFlex being equal in each flexibility demand scenario as the booked LongFlex variable only is dependent on time. Meaning that the cost of booking and activating LongFlex is cheaper than activating ShortFlex in these time steps, and the optimization model therefore books enough LongFlex to cover the highest flexibility demand across the three flexibility demand scenarios.

Flexibility and Discharge

Figure 5.7 presents the flexibility demand and the second stage battery discharge for each of the three flexibility demand scenarios, and for both cost of flexibility profiles. Figure 5.7a presents the result from cost of flexibility profile 1 and figure 5.7b presents the results from cost of flexibility profile 2.



(a) Flexibility demand scenario 1, 2 and 3 using cost profile 1.



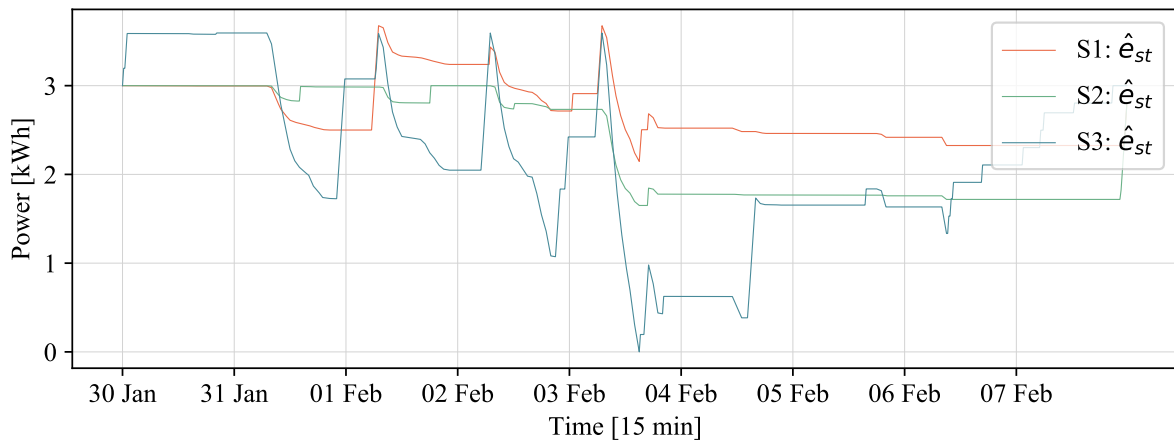
(b) Flexibility demand scenario 1, 2 and 3 using cost profile 2.

Figure 5.7: Flexibility demand and second stage battery discharge for each flexibility demand scenario for the various cost profiles.

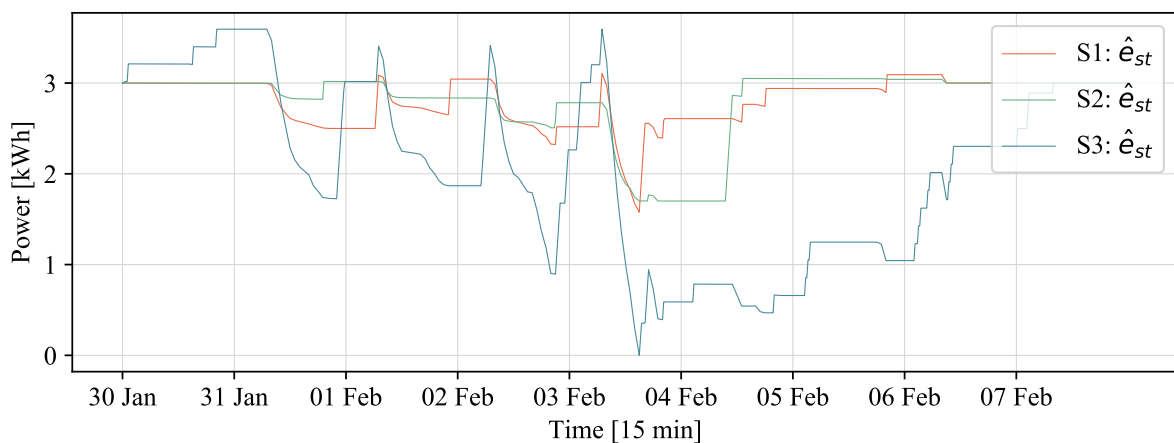
The flexibility demand is the same for both of the cost of flexibility profiles, as it is a given parameter in the optimization model. However, it can be observed from figure 5.7a and figure 5.7b that the second stage battery discharge matches the flexibility demand in each flexibility demand scenario and both cost of flexibility profiles. This acts as a verification of the optimization model, as the model uses the battery to procure the necessary flexibility to cover the flexibility demand in each flexibility scenario.

Second Stage Battery SOC

The second stage battery SOC for each flexibility demand and for both cost of flexibility profiles are presented in figure 5.8. The results for cost of flexibility profile 1 are presented in figure 5.8a and for cost of flexibility profile 2 in figure 5.8b. It can be observed that the second stage battery SOC begins at 3 kWh for all of the flexibility demand scenarios across the cost of flexibility profiles. This is because the second stage battery SOC was set to 3 kWh for all $t = 0$. Thereby creating an equal starting point across all scenarios.



(a) Flexibility demand scenario 1, 2 and 3.



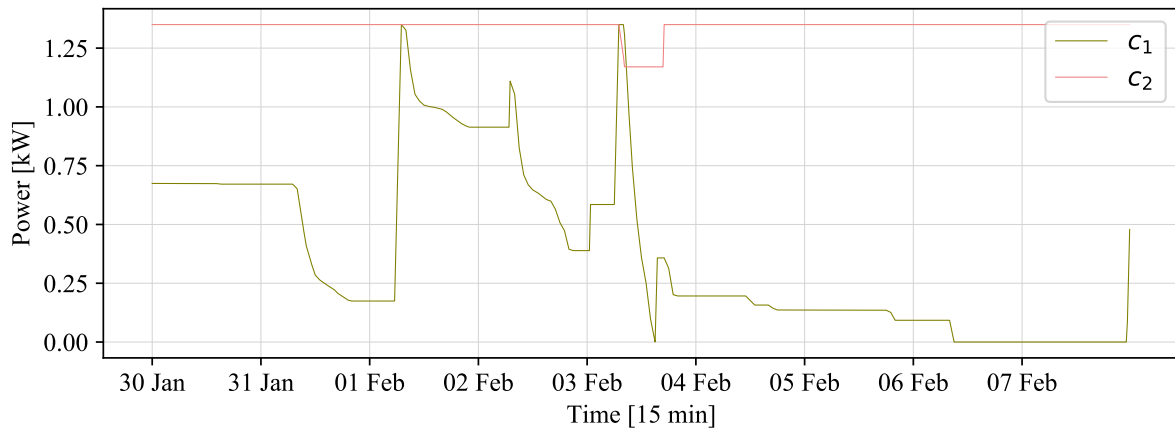
(b) Flexibility demand scenario 1, 2 and 3.

Figure 5.8: Second stage battery SOC for each cost profile.

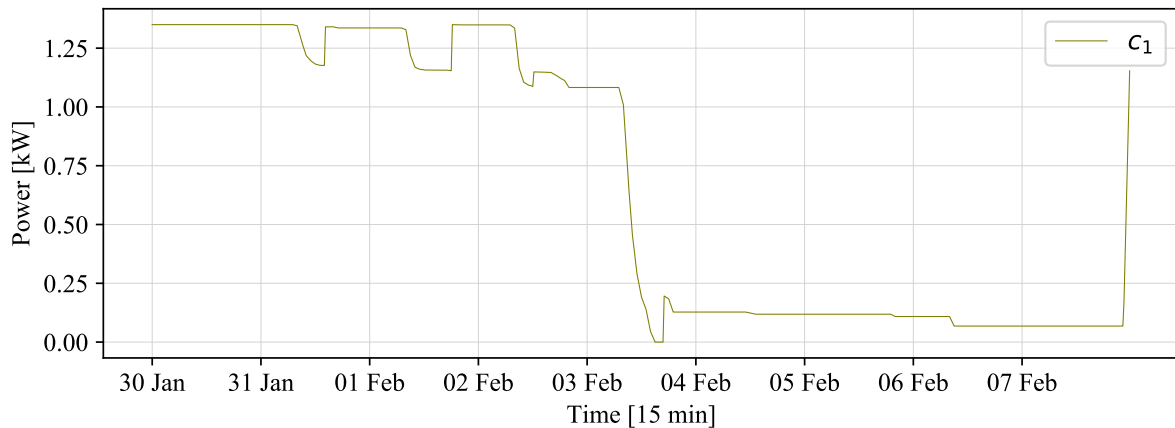
By comparing figure 5.8a and 5.8b it can be observed that the amount of discharge in each time step across the same flexibility demand scenarios for both cost of flexibility profiles are equal. The difference is in the charging, as it is up to the optimization model to decide. The only constraints regarding the charging is the maximum amount allowed to be charged every 15 minutes and that charging cannot happen in a time step with discharge. As there are many time steps without flexibility demand in each scenario, the second stage battery charging variable has several options for charging.

Second Stage Battery SOC Segment

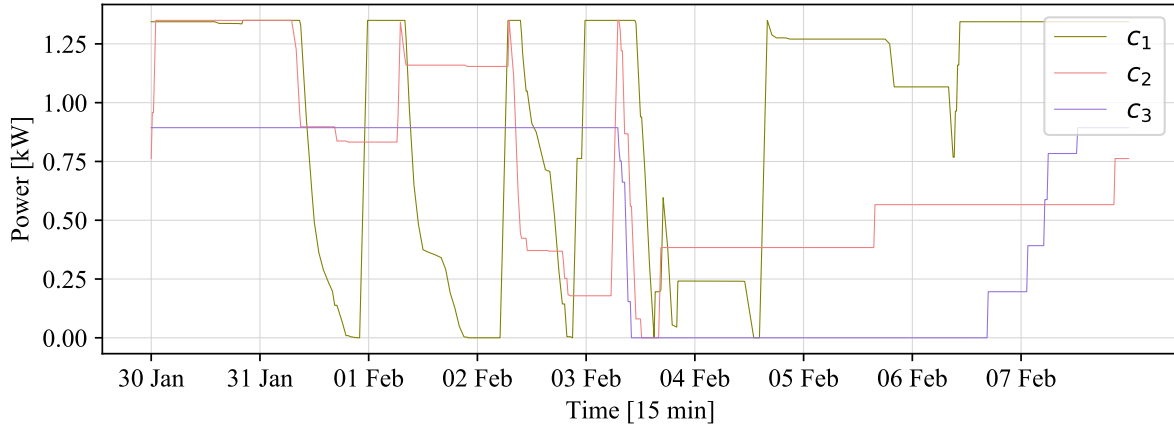
The second stage battery SOC per segment for each flexibility demand scenario using cost of flexibility scenario 1 are presented in figure 5.9. The results from flexibility demand scenario 1 are presented in figure 5.9a, from flexibility demand scenario 2 are presented in figure 5.9b and flexibility demand scenario 3 are presented in figure 5.9c. It can be observed from figure 5.9b that flexibility demand scenario 2, which is the lowest, results in only the use of battery segment 1. While flexibility demand scenario 3, figure 5.9c, which is the highest, uses three battery segments.



(a) Flexibility demand scenario 1.



(b) Flexibility demand scenario 2.

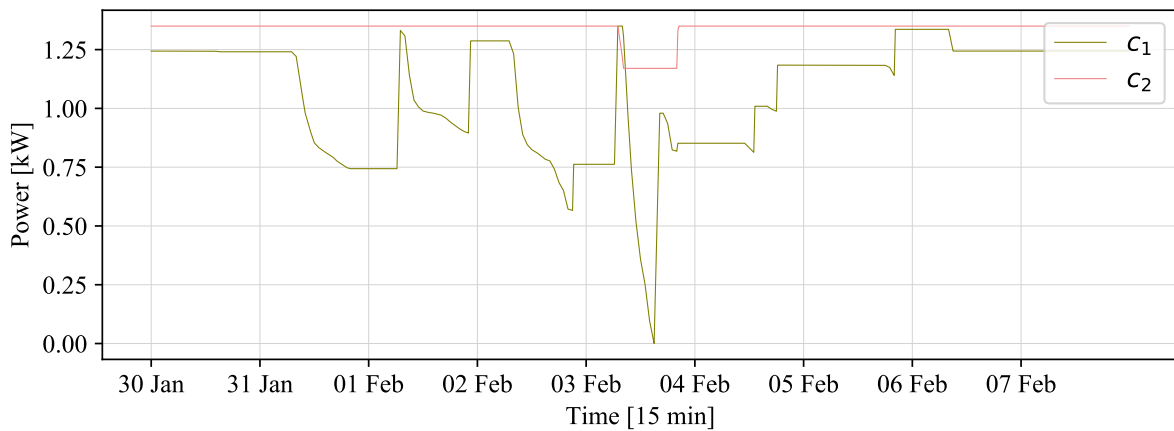


(c) Flexibility demand scenario 3.

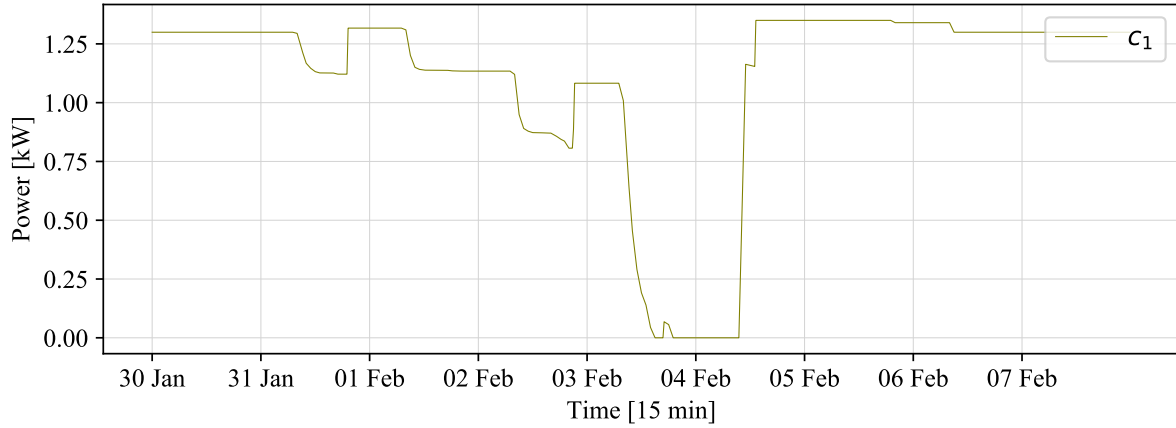
Figure 5.9: Second stage battery segment SOC for cost of flexibility profile 1.

Further, by comparing the three figures it can also be observed that the initial starting point of each segment varies between the three flexibility scenarios. This is a result of no set initial state. There are no additional constraint set for the charging of the segments, so the model is free to choose from several possible charging patterns. In some instances the charging is not necessary, for example at the end of the time period when there is no more discharging, however, this does not matter as there are not set cost of charging.

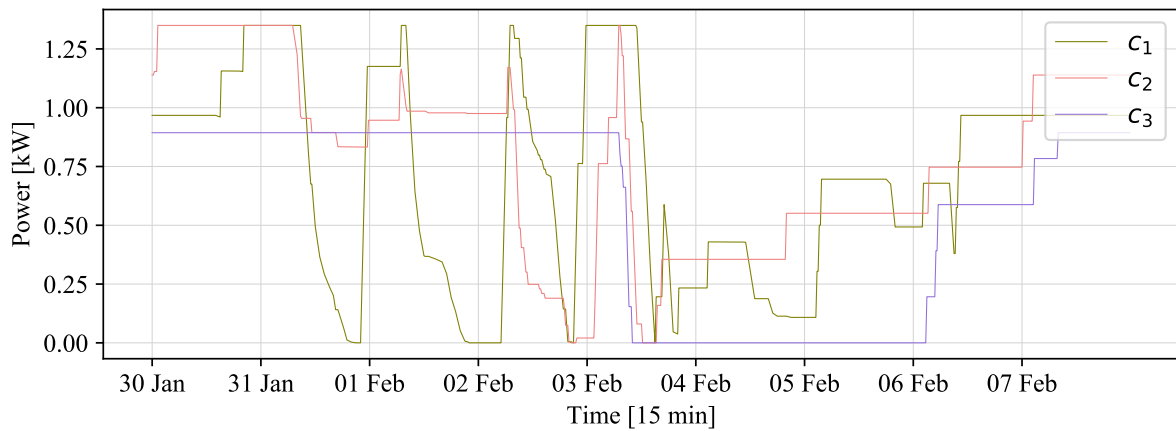
Figure 5.10 presents the second stage battery segments SOC for each flexibility demand scenario using cost of flexibility profile 2. The results from flexibility demand scenario 1 are presented in figure 5.10a, results from flexibility demand scenario 2 are presented in figure 5.10b and results from flexibility demand scenario 3 are presented in figure 5.10c. By comparing these results with cost profile 1, presented in figure 5.9, it can be observed that the same battery segments are used for the same flexibility demand scenarios. The discharging is the same, however, the charging varies. In figure 5.10c it can be observed that the deepest segment used, c_3 , is only activated when segments, c_1 and c_2 , are fully discharged.



(a) Flexibility demand scenario 1.



(b) Flexibility demand scenario 2.



(c) Flexibility demand scenario 3.

Figure 5.10: Second stage battery segment SOC for cost of flexibility profile 2.

Distribution System Operator Costs

Table 5.1 presents the total costs for booking and activating LongFlex, activating ShortFlex and battery degradation for cost of flexibility profile 1 and 2. Firstly, it can be observed that the cost of battery degradation is the same for both cost profiles. This is expected as the same amount of power is discharged in both scenarios and the same segments are used. The cost of degradation is quite low, however, this is a result of operating with small amounts of power. Further, the battery used has a greater capacity than necessary and the use of the battery segments are therefore limited to the cheapest segments. It could also be argued that the cost of degradation is not a cost that should be considered as “belonging” to the DSO. However, the cost of degradation must be covered by the battery owner and it is possible to assume that this cost must be partly or fully covered by the flexibility buyer.

Table 5.1: *Distribution system operator costs per cost of flexibility profile.*

Cost	Profile 1	Profile 2
Booking LongFlex	0.3999 NOK	0.3649 NOK
Activating LongFlex	2.5995 NOK	1.2458 NOK
Activation ShortFlex	5.6057 NOK	6.1326 NOK
Battery degradation	0.3941 NOK	0.3941 NOK
Total	8.9992 NOK	8.1374 NOK

The total cost of booking and activating LongFlex and activating ShortFlex do vary between the to cost profiles for flexibility. This is expected as two various cost profiles are used, however, the variation in cost profile 2 also effects this as the cost of activating LongFlex and ShortFlex vary a lot. The total costs of booking and activating flexibility are also quite low. This is also a result of operating with small amounts of power. The total cost for the DSO as a result of both of the two cost profiles are low. However, in a distribution system with greater flexibility demands and greater battery system, the costs will increase. In addition, it could be assumed that the costs of flexibility will be higher than the costs used here.

5.2.2 Power Quality

The use of the flexibility demand procured by using the power quality voltage limits, for both cost of flexibility profiles results in an infeasible optimization model. This is a result of the flexibility demand being to great. The constant flexibility demand in each time step results in no opportunities for the battery to charge, as discharging and charging can not happen at the same time. One solution to this is to use several batteries in the network, so that one battery can charge while the other discharge. However, in a network with a constant flexibility demand it might be an option use other methods to reinforce the grid.

5.2.3 Optimization Model

The optimization model does not account for how the additional power in the network from available charging power and power from battery discharging effects the system. The optimization model only secures that the flexibility demand is met and that the battery has power to charge. The additional power in network might cause overloading of the transformer or the lines, as well as new voltage-issues at the buses. This could be solved by procuring the flexibility demand through optimal power flow by e.g. install generators as batteries. The generator will then generated the amount of flexibility needed to maintain set voltage limits. By using optimal power flow it is also possible to ensure that there are no overloading issues at the transformer or at any lines, and that the buses have a voltage within set limits. However, even though optimal power flow results in a more accurate flexibility demand, it can also be argued that the DSO will not buy 1 kW from the LFM and then check the effect of this on the grid before buying more, which is an effect of using optimal power flow to procure the flexibility demand.

Chapter 6

Conclusion

This master thesis presents two models. The first model is a network model of the case study network. The results from the power flow time series simulations of the network model, using the three load profile scenarios, leads to long and very long under-voltage issues. Two various voltage limits were set, under-voltage at 0.9 pu and power quality at 0.95, to investigate the violations in the various load profile scenarios and the flexibility needed to avoid these violations. The varying load profile scenarios and the two voltage limits results in a varying amount of load buses with violations, a varying amount of violations and a varying amount of time periods with violations.

From the results in the network model three flexibility demands were obtained for each voltage limit. In addition, two cost of flexibility profiles were created for the use in the two-stage optimization model. By using the flexibility demands acquired from the use of the under-voltage limit in the optimization model it was verified that optimization model operated as it should. The optimization model booked and activated enough flexibility to cover the scenario based flexibility demands, and discharged this amount of flexibility in second stage.

Further, the use of the various cost profiles in the model resulted in various use of LongFlex and ShortFlex. In time steps with flexibility demand across all three flexibility demand scenarios, LongFlex was booked and activated if the total cost of this was lower than the cost of activating ShortFlex in all three scenarios. In cost of flexibility profile 2 this varied due to a varying cost profile. However, in scenario 1 the cost of booking and activating LongFlex was equal to the cost of activating ShortFlex. The optimization model therefore booked LongFlex to reduce the costs in the time steps with flexibility demand across the three scenarios.

Even though the battery used in the optimization model has 10 segments, the maximum amount of segments used were three. This is because the battery was overdimensioned. The use of various cost profiles resulted in various charging patterns, as the charging was not very restricted, however, the discharging patterns were the same. The total costs for DSO were quite low, as a result of only using the cheapest segments in the battery due to it being overdimensioned and operating with small amounts of kWh. In addition, the two cost profiles do not represent actual costs of flexibility, which might be higher. In a distribution system with greater flexibility demands and greater battery system, the costs will increase.

The use of the flexibility demands procured using the power quality limit resulted in an infeasible optimization model. This was due to a constant demand and thereby no opportunities for the battery to charge. In cases with power quality in mind the options are either to increase the total amount of battery capacity, increase the amount of batteries or reinforce the grid in other ways.

After evaluating all the results it can be concluded that the weakening of the case study network resulted in a varying degree of under-voltage issues for the three load profile scenarios, leading to various flexibility demand scenarios. Further, the two-stage optimization model acts as it should, procuring the necessary flexibility through a battery, while minimizing the costs for the DSO. In addition, it can be concluded that it is possible to use batteries for voltage control, however, in situations with a great flexibility demand other methods should also be considered. In situations where using batteries the cost of battery degradation must also be considered, as it does increase the total cost for the DSO.

Further Work

The method used for procuring the flexibility demands is quite simple and it does not take into account how previously acquired flexibility might effect the flexibility demand. It might therefore be advantageous to use optimal power flow to acquire the flexibility demand. Further, the two-stage optimization model does not account for how “injected” power into the network from discharging of the battery and power for charging might effect the system. By using optimal power flow to procure the flexibility demand, such issues can be avoided. A model for procuring the flexibility demand through optimal power flow should therefore be made for comparison.

Some work should also be put into investigating the what the optimal size of the battery to use is in the model dependent one the flexibility demand is. An overdimensioned battery offers the use of only the cheapest segments, however, it will lead to unnecessary investment costs. This optimization model should therefore also be used with various battery sizes to investigate the optimal battery size. It would also be interesting to see how this effects the total cost for DSO.

This optimization model focuses on minimizing the DSO cost, however, there should be put some thought into the charging of the battery. In this model the battery charging is not very restricted, however, the owner of the battery must pay a cost for charging the battery using the grid. This cost will change the charging patterns and thereby effect the DSO’s access to the battery, at least for the use of ShortFlex.

In a situation considering the power quality it should be investigated if it is more cost effective to reinforce the grid in other ways or use flexibility from several batteries. It could also be interesting to see how PV in the network model might effect the power quality demand for flexibility.

References

- [1] Unknown, *Decentralized energy system*, (Accessed on 20/04/2022). [Online]. Available: <https://www.unescap.org/sites/default/files/14.\%20FS-Decentralized-energy-system.pdf>.
- [2] J. Villar, R. Bessa, and M. Matos, “Flexibility products and markets: Literature review,” *Electric Power Systems Research*, vol. 154, pp. 329–340, 2018, ISSN: 0378-7796. DOI: <https://doi.org/10.1016/j.epsr.2017.09.005>. [Online]. Available: <https://www.sciencedirect.com/science/article/pii/S0378779617303723>.
- [3] X. Jin, Q. Wu, and H. Jia, “Local flexibility markets: Literature review on concepts, models and clearing methods,” *Applied Energy*, vol. 261, p. 114387, 2020, ISSN: 0306-2619. DOI: <https://doi.org/10.1016/j.apenergy.2019.114387>. [Online]. Available: <https://www.sciencedirect.com/science/article/pii/S0306261919320744>.
- [4] Lovdata, *Forskrift om leveringskvalitet i kraftsystemet*, (Accessed on 04/04/2022). [Online]. Available: <https://lovdata.no/dokument/LTI/forskrift/2004-11-30-1557>.
- [5] J. Petinrin and M. Shaaban, “Impact of renewable generation on voltage control in distribution systems,” *Renewable and Sustainable Energy Reviews*, vol. 65, pp. 770–783, 2016, ISSN: 1364-0321. DOI: <https://doi.org/10.1016/j.rser.2016.06.073>. [Online]. Available: <https://www.sciencedirect.com/science/article/pii/S1364032116303094>.
- [6] D. GL, “Batterier i distribusjonsnettene,” 2017. [Online]. Available: https://publikasjoner.nve.no/rapport/2018/rapport2018_02.pdf.
- [7] *Recast electricity directive - legiswrite*, (Accessed on 05/24/2022). [Online]. Available: https://eur-lex.europa.eu/resource.html?uri=cellar:c7e47f46-faa4-11e6-8a35-01aa75ed71a1.0014.02/DOC_1&format=PDF.
- [8] R. H. Berge, “Reducing voltage related challenges through flexibility and modelling of a distribution grid,” 2021, Specialization project, NTNU.
- [9] EnergifaktaNorge, *Strømnettet*, (Accessed on 19/03/2022). [Online]. Available: <https://energifaktanorge.no/norsk-energiforsyning/kraftnett/>.
- [10] J. Bjørndalen, I. B. Løken, C. L. Berntsen, R. B. Bjørkli, I. Gimmetad, and K. Sletten, “Fra brettet til det smarte nettet – Ansvar for driftskoordinering i kraftsystemet,” p. 86, 2020.
- [11] NVE, *The norwegian power system; grid connection and licensing*, (Accessed on 18/03/2022), 2018. [Online]. Available: https://publikasjoner.nve.no/faktaark/2018/faktaark2018_03.pdf.
- [12] EnergiNorge, *DSO*, (Accessed on 28/03/2022). [Online]. Available: <https://www.energinorge.no/tall-og-fakta/ordbok2/dso/>.
- [13] EnergifaktaNorge, *Regulering av nettvirksomheten*, (Accessed on 23/03/2022). [Online]. Available: <https://energifaktanorge.no/regulering-av-energisektoren/regulering-av-nettvirksomhet/>.

- [14] NVE, *Forskrift om leveringskvalitet - nve*, (Accessed on 12/04/2022). [Online]. Available: <https://www.nve.no/reguleringsmyndigheten/regulering/nettvirksomhet/leveringskvalitet/forskrift-om-leveringskvalitet/>.
- [15] *Centralized generation of electricity and its impacts on the environment — us epa*, (Accessed on 20/04/2022). [Online]. Available: <https://www.epa.gov/energy/centralized-generation-electricity-and-its-impacts-environment>.
- [16] EPA, *Distributed generation of electricity and its environmental impacts*, (Accessed on 19/04/2022). [Online]. Available: <https://www.epa.gov/energy/distributed-generation-electricity-and-its-environmental-impacts>.
- [17] A. Patwardhan, I. Azevedo, T. Foran, *et al.*, “Transitions in energy systems. chapter 16,” in Jan. 2012.
- [18] H. Ibrahim, A. Ilinca, and J. Perron, “Energy storage systems—characteristics and comparisons,” *Renewable and Sustainable Energy Reviews*, vol. 12, no. 5, pp. 1221–1250, 2008, ISSN: 1364-0321. DOI: <https://doi.org/10.1016/j.rser.2007.01.023>. [Online]. Available: <https://www.sciencedirect.com/science/article/pii/S1364032107000238>.
- [19] L. Kristov, “The bottom-up (r)evolution of the electric power system: The pathway to the integrated-decentralized system,” *IEEE Power and Energy Magazine*, vol. 17, no. 2, pp. 42–49, 2019. DOI: 10.1109/MPE.2018.2885204.
- [20] NVE, *Network tariffs*, (Accessed on 22/04/2022). [Online]. Available: <https://2021.nve.no/norwegian-energy-regulatory-authority/network-regulation/network-tariffs/>.
- [21] P. Palensky and D. Dietrich, “Demand side management: Demand response, intelligent energy systems, and smart loads,” *IEEE Transactions on Industrial Informatics*, vol. 7, no. 3, pp. 381–388, 2011. DOI: 10.1109/TII.2011.2158841.
- [22] M. H. Albadi and E. F. El-Saadany, “Demand response in electricity markets: An overview,” pp. 1–5, 2007. DOI: 10.1109/PES.2007.385728.
- [23] A. M. Attia, K. H. Youssef, and N. H. Abbasy, “A comparative analysis and simulation of load shaping techniques,” pp. 664–669, 2018. DOI: 10.1109/PowerAfrica.2018.8521019.
- [24] I. Diaz de Cerio Mendaza, “An interactive energy system with grid, heating and transportation systems,” English, Ph.D. dissertation, Oct. 2014, ISBN: 978-87-92846-42-6.
- [25] T. Ackermann and V. Knyazkin, “Interaction between distributed generation and the distribution network: Operation aspects,” in *IEEE/PES Transmission and Distribution Conference and Exhibition*, vol. 2, 2002, 1357–1362 vol.2. DOI: 10.1109/TDC.2002.1177677.
- [26] M. A. Masoum and E. F. Fuchs, “Chapter 1 - introduction to power quality,” in *Power Quality in Power Systems and Electrical Machines (Second Edition)*, M. A. Masoum and E. F. Fuchs, Eds., Second Edition, Boston: Academic Press, 2015, pp. 1–104, ISBN: 978-0-12-800782-2. DOI: <https://doi.org/10.1016/B978-0-12-800782-2.00001-4>. [Online]. Available: <https://www.sciencedirect.com/science/article/pii/B978012800782200014>.

- [27] M. F. McGranaghan, S. Santoso, R. C. Dugan, and H. W. Beaty, “Chapter 7 - long-duration voltage variations,” in *Electrical Power Systems Quality (Third Edition)*, McGraw-Hill Professional, 2012, ISBN: 0-07-176155-1. DOI: 10.1036/9780071761567.
- [28] K. E. Antoniadou-Plytaria, I. N. Kouveliotis-Lysikatos, P. S. Georgilakis, and N. D. Hatziaargyriou, “Distributed and decentralized voltage control of smart distribution networks: Models, methods, and future research,” *IEEE Transactions on Smart Grid*, vol. 8, no. 6, pp. 2999–3008, 2017. DOI: 10.1109/TSG.2017.2679238.
- [29] N. Mahmud and A. Zahedi, “Review of control strategies for voltage regulation of the smart distribution network with high penetration of renewable distributed generation,” *Renewable and Sustainable Energy Reviews*, vol. 64, pp. 582–595, 2016, ISSN: 1364-0321. DOI: <https://doi.org/10.1016/j.rser.2016.06.030>. [Online]. Available: <https://www.sciencedirect.com/science/article/pii/S136403211630243X>.
- [30] A. Ciocia, V. A. Boicea, G. Chicco, P. D. Leo, A. Mazza, and et al., “Voltage control in low-voltage grids using distributed photovoltaic converters and centralized devices,” pp. 225–237, 2019. [Online]. Available: <https://hal.archives-ouvertes.fr/hal-02350955/document>.
- [31] O. Babatunde, J. Munda, and Y. Hamam, “Power system flexibility: A review,” *Energy Reports*, vol. 6, pp. 101–106, 2020, The 6th International Conference on Power and Energy Systems Engineering, ISSN: 2352-4847. DOI: <https://doi.org/10.1016/j.egy.2019.11.048>. [Online]. Available: <https://www.sciencedirect.com/science/article/pii/S2352484719309242>.
- [32] M. Z. Degefa, I. B. Sperstad, and H. Sæle, “Comprehensive classifications and characterizations of power system flexibility resources,” *Electric Power Systems Research*, vol. 194, p. 107022, 2021, ISSN: 0378-7796. DOI: <https://doi.org/10.1016/j.epsr.2021.107022>. [Online]. Available: <https://www.sciencedirect.com/science/article/pii/S037877962100002X>.
- [33] C. Eid, P. Codani, Y. Perez, J. Reneses, and R. Hakvoort, “Managing electric flexibility from distributed energy resources: A review of incentives for market design,” *Renewable and Sustainable Energy Reviews*, vol. 64, pp. 237–247, 2016, ISSN: 1364-0321. DOI: <https://doi.org/10.1016/j.rser.2016.06.008>. [Online]. Available: <https://www.sciencedirect.com/science/article/pii/S1364032116302222>.
- [34] K. Kouzelis, B. Bak-Jensen, and J. R. Pillai, “The geographical aspect of flexibility in distribution grids,” in *2015 IEEE Power Energy Society Innovative Smart Grid Technologies Conference (ISGT)*, 2015, pp. 1–5. DOI: 10.1109/ISGT.2015.7131888.
- [35] *Centralised and distributed optimization for aggregated flexibility services provision - scientific figure on researchgate*, (Accessed on 28/05/2022). [Online]. Available: https://www.researchgate.net/figure/Local-flexibility-market-framework_fig1_339019120.
- [36] NODES, *About*, (Accessed on 28/05/2022). [Online]. Available: <https://nodesmarket.com/about/>.
- [37] —, *Shortflex*, (Accessed on 28/05/2022). [Online]. Available: <https://nodesmarket.com/shortflex/>.

- [38] —, *Longflex*, (Accessed on 28/05/2022). [Online]. Available: <https://nodesmarket.com/longflex/>.
- [39] I. Birkeland, L. Fløtre I. Bergland, and O. Skeie, “Batterier i distribusjonsnettet,” 2020. [Online]. Available: <https://publikasjoner.nve.no/diverse/2020/batterier.i.distribusjonsnettet.pdf>.
- [40] M. Koller, T. Borsche, A. Ulbig, and G. Andersson, “Defining a degradation cost function for optimal control of a battery energy storage system,” in *2013 IEEE Grenoble Conference*, 2013, pp. 1–6. DOI: 10.1109/PTC.2013.6652329.
- [41] B. Xu, A. Oudalov, A. Ulbig, G. Andersson, and D. S. Kirschen, “Modeling of lithium-ion battery degradation for cell life assessment,” *IEEE Transactions on Smart Grid*, vol. 9, no. 2, pp. 1131–1140, 2018. DOI: 10.1109/TSG.2016.2578950.
- [42] A. Alhamali, M. E. Farrag, G. Bevan, and D. M. Hepburn, “Review of energy storage systems in electric grid and their potential in distribution networks,” in *2016 Eighteenth International Middle East Power Systems Conference (MEPCON)*, 2016, pp. 546–551. DOI: 10.1109/MEPCON.2016.7836945.
- [43] B. Xu, J. Zhao, T. Zheng, E. Litvinov, and D. S. Kirschen, “Factoring the cycle aging cost of batteries participating in electricity markets,” *IEEE Transactions on Power Systems*, vol. 33, no. 2, pp. 2248–2259, 2018. DOI: 10.1109/TPWRS.2017.2733339.
- [44] P. Akkaş and E. Çam, “Optimal operational scheduling of a virtual power plant participating in day-ahead market with consideration of emission and battery degradation cost,” *International Transactions on Electrical Energy Systems*, vol. 30, no. 7, e12418, 2020, eprint: <https://onlinelibrary.wiley.com/doi/pdf/10.1002/2050-7038.12418>. DOI: <https://doi.org/10.1002/2050-7038.12418>. [Online]. Available: <https://onlinelibrary.wiley.com/doi/abs/10.1002/2050-7038.12418>.
- [45] C. Bordin, H. O. Anuta, A. Crossland, I. L. Gutierrez, C. J. Dent, and D. Vigo, “A linear programming approach for battery degradation analysis and optimization in offgrid power systems with solar energy integration,” *Renewable Energy*, vol. 101, pp. 417–430, 2017, ISSN: 0960-1481. DOI: <https://doi.org/10.1016/j.renene.2016.08.066>. [Online]. Available: <https://www.sciencedirect.com/science/article/pii/S0960148116307765>.
- [46] S. Bjarghov, M. Kalantar-Neyestanaki, R. Cherkaoui, and H. Farahmand, “Battery degradation-aware congestion management in local flexibility markets,” in *2021 IEEE Madrid PowerTech*, Madrid, Spain: IEEE, Jun. 28, 2021, pp. 1–6, ISBN: 978-1-66543-597-0. DOI: 10.1109/PowerTech46648.2021.9494829. [Online]. Available: <https://ieeexplore.ieee.org/document/9494829/> (visited on 11/15/2021).
- [47] E. Haugen, K. Berg, B. N. Torsæter, and M. Korpås, “Optimisation model with degradation for a battery energy storage system at an ev fast charging station,” in *2021 IEEE Madrid PowerTech*, 2021, pp. 1–6. DOI: 10.1109/PowerTech46648.2021.9494979.
- [48] M. Albadi, *Power flow analysis, computational models in engineering*, (Accessed on 28/04/2022), Mar. 2019. [Online]. Available: <https://www.intechopen.com/books/computational-models-in-engineering/power-flow-analysis>.
- [49] M.-H. Hadi Saadat, *Power System Analysis*, ser. McGraw Hill Series in Electrical and Computer Engineering. 1999.

- [50] J. D. Glover, T. J. Overbye, and M. S. Sarma, *Power System Analysis and Design*, 6th ed. Cengage Learning, 2017, ISBN: 978-1-305-63213-4.
- [51] C. Li and I. E. Grossmann, “A review of stochastic programming methods for optimization of process systems under uncertainty,” 2021, (Accessed on 01/05/2022). [Online]. Available: <https://www.frontiersin.org/articles/10.3389/fceng.2020.622241/full>.
- [52] IEEE, *Resources – ieee pes test feeder*, (Accessed on 25/02/2022). [Online]. Available: <https://cmte.ieee.org/pes-testfeeders/resources/>.
- [53] S. Zaferanlouei, M. Korpås, H. Farahmand, and V. Vadlamudi, “Integration of pev and pv in norway using multi-period acopf — case study,” pp. 1–6, Jun. 2017. DOI: 10.1109/PTC.2017.7981042.
- [54] L. Thurner, A. Scheidler, F. Schäfer, *et al.*, “Pandapower — an open-source python tool for convenient modeling, analysis, and optimization of electric power systems,” *IEEE Transactions on Power Systems*, vol. 33, no. 6, pp. 6510–6521, Nov. 2018, ISSN: 0885-8950. DOI: 10.1109/TPWRS.2018.2829021.
- [55] Pandapower, *About pandapower*, (Accessed on 10/03/2022), 2021. [Online]. Available: <http://www.pandapower.org/about/>.
- [56] F. IEE and U. of Kassel, *Pandapower documentation: Timeseries module overview*, (Accessed on 10/03/2022). [Online]. Available: https://pandapower.readthedocs.io/en/stable/timeseries/timeseries_loop.html.
- [57] L. Herenčić, P. Ilak, and I. Rajšl, “Effects of local electricity trading on power flows and voltage levels for different elasticities and prices,” *Energies*, vol. 12, no. 24, 2019, ISSN: 1996-1073. DOI: 10.3390/en12244708. [Online]. Available: <https://www.mdpi.com/1996-1073/12/24/4708>.
- [58] W. E. Hart, J.-P. Watson, and D. L. Woodruff, “Pyomo: Modeling and solving mathematical programs in python,” 2011.
- [59] Gurobi, *Gurobi optimizer*, (Accessed on 03/03/2022). [Online]. Available: <https://www.gurobi.com/products/gurobi-optimizer/>.
- [60] N. Pool, *Market data*, (Accessed on 07/06/2022). [Online]. Available: <https://www.nordpoolgroup.com/en/Market-data1/Dayahead/Area-Prices/ALL1/Hourly/?view=table>.
- [61] Sonnen, (Accessed on 02/06/2022). [Online]. Available: <https://midsummerwholesale.co.uk/pdfs/sonnen-953-datasheet.pdf>.
- [62] M. Energy, *Sonnen hybrid 9.53*, (Accessed on 07/06/2022). [Online]. Available: <https://midsummerwholesale.co.uk/buy/sonnen/sonnen-hybrid-953-eco9-screen-kits>.

Appendix A

Network Model Data

This appendix presents all relevant data used in the network model, such as line connections, line types- and transformer specifications.

A.1 Line Connections

Table A.1: *Presentation of line connections, line lengths and line types. Based on [52].*

From	To	Length [km]	Type
1	2	0.2333	4c ₇₀
2	3	0.0416	2c _{.007}
2	4	0.0782	4c ₇₀
4	5	0.0885	2c ₁₆
5	6	0.0803	2c ₁₆
5	7	0.1013	2c ₁₆
4	8	0.1893	4c ₇₀
8	9	0.0860	2c ₁₆
9	10	0.0966	2c ₁₆
9	11	0.0923	2c ₁₆
8	12	0.12	4c ₇₀
12	13	0.5753	4c ₁₈₅
12	14	0.1467	4c ₇₀
14	15	0.0192	4c ₇₀
14	16	0.0503	4c ₇₀
16	17	0.1239	2c ₁₆
17	18	0.0606	2c ₁₆
17	19	0.0606	2c ₁₆
1	20	0.2007	4c ₇₀
20	21	0.2202	4c _{.35}

21	22	0.2781	$2c_{16}$
21	23	0.1845	$4c_{.35}$
23	24	0.2121	$4c_{.35}$
24	25	0.2769	$2c_{16}$
23	26	0.1868	$2c_{16}$
26	27	0.1037	$2c_{16}$
26	28	0.1236	$2c_{16}$
23	29	0.111	$4c_{.35}$
29	30	0.2043	$2c_{16}$
30	31	0.0795	$2c_{16}$
30	32	0.0795	$2c_{16}$
29	33	0.017	$4c_{.35}$
33	34	0.132	$4c_{70}$
1	35	0.2007	$4c_{70}$
35	36	0.0498	$2c_{.007}$
35	37	0.0465	$4c_{.35}$
37	38	0.2153	$2c_{16}$
37	39	0.2415	$4c_{.35}$
39	40	0.1679	$2c_{16}$
40	41	0.1032	$2c_{16}$
40	42	0.072	$2c_{16}$
39	43	0.2451	$4c_{.35}$
43	44	0.1562	$2c_{16}$
44	45	0.1068	$2c_{16}$
44	46	0.05	$2c_{16}$
43	47	0.0677	$4c_{.35}$
47	48	0.0487	$4c_{.35}$
47	49	0.0521	$4c_{.35}$

A.2 Line Types Specifications

Table A.2: Presentation of the line type specifications. Based on [52].

Type	Line resistance	Line inductance	Line capacitance	Max thermal
	[Ω /km]	[Ω /km]	[nF/km]	current [kA]
2c _{.007}	3.97	0.099	1	0.105
2c _{.0225}	1.257	0.085	1	0.14
2c ₁₆	1.15	0.088	1	0.14
35 _{SACXSC}	0.868	0.092	1	0.17
4c _{.06}	0.469	0.075	1	0.217
4c _{.1}	0.274	0.073	1	0.28
4c _{.35}	0.089	0.0675	1	0.74
4c ₁₈₅	0.166	0.068	1	0.362
4c ₇₀	0.446	0.071	1	0.217
4c _{95SACXC}	0.322	0.074	1	0.249

A.3 Transformer Specifications

Table A.3: Transformer specifications. Based on [52].

Parameters	Value
Rated apparent power	0.8 MVA
Rated high voltage	11 kV
Rated low voltage	0.23 kV
Short circuit voltage	4.0 %
Real component of short circuit voltage	1.0794 %
Iron losses	1.18 kW
Open loop losses	0.1873 %
Transformer phase shift angle	150°

